


RESEARCH ARTICLE

Temporal changes in the microglial proteome of male and female mice after a diffuse brain injury using label-free quantitative proteomics

Yasmine V. Doust¹ | Aidan Bindoff¹ | Olivia G. Holloway¹ | Richard Wilson² | Anna E. King¹ | Jenna M. Ziebell¹ 

¹Wicking Dementia Research and Education Centre, College of Health and Medicine, University of Tasmania, Hobart, Tasmania, Australia

²Central Science Laboratory (CSL), University of Tasmania, Hobart, Tasmania, Australia

Correspondence

Jenna M. Ziebell, Wicking Dementia Research and Education Centre, College of Health and Medicine, University of Tasmania, Hobart, Tasmania 7001, Australia.
Email: jenna.ziebell@utas.edu.au

Funding information

JO and JR Wicking trust; National Health and Medical Research Council, Grant/Award Number: APP1136913

Abstract

Traumatic brain injury (TBI) triggers neuroinflammatory cascades mediated by microglia, which promotes tissue repair in the short-term. These cascades may exacerbate TBI-induced tissue damage and symptoms in the months to years post-injury. However, the progression of the microglial function across time post-injury and whether this differs between biological sexes is not well understood. In this study, we examined the microglial proteome at 3-, 7-, or 28-days after a mid-line fluid percussion injury (mFPI) in male and female mice using label-free quantitative proteomics. Data are available via ProteomeXchange with identifier PXD033628. We identified a reduction in microglial proteins involved with clearance of neuronal debris via phagocytosis at 3- and 7-days post-injury. At 28 days post-injury, pro-inflammatory proteins were decreased and anti-inflammatory proteins were increased in microglia. These results indicate a reduction in microglial clearance of neuronal debris in the days post-injury with a shift to anti-inflammatory function by 28 days following TBI. The changes in the microglial proteome that occurred across time post-injury did not differ between biological sexes. However, we did identify an increase in microglial proteins related to pro-inflammation and phagocytosis as well as insulin and estrogen signaling in males compared with female mice that occurred with or without a brain injury. Although the microglial response was similar between males and females up to 28 days following TBI, biological sex differences in the microglial proteome, regardless of TBI, has implications for the efficacy of treatment strategies targeting the microglial response post-injury.

KEYWORDS

biological sex, inflammation, microglia, proteomics, TBI, traumatic brain injury

Anna E. King and Jenna M. Ziebell contributed equally to this work and share senior authorship.

This is an open access article under the terms of the [Creative Commons Attribution-NonCommercial](https://creativecommons.org/licenses/by-nc/4.0/) License, which permits use, distribution and reproduction in any medium, provided the original work is properly cited and is not used for commercial purposes.

© 2022 The Authors. GLIA published by Wiley Periodicals LLC.

1 | INTRODUCTION

Traumatic brain injury (TBI) is a neurological condition that can result in clinical symptoms that include cognitive deficits, memory impairments and sensorimotor dysfunction (de Freitas Cardoso et al., 2019; Galea et al., 2018). The severity of TBI can range from mild to severe, where 80% of TBI cases that present to the clinic are mild to moderate; sustained mostly from falls, motor vehicle accidents and assault (Dhandapani et al., 2012; Laskowski et al., 2015). At the time of injury, mechanical damage occurs to the brain due to movement of the brain within the skull which triggers secondary injury cascades that continue for days to months following TBI (Prins et al., 2013). Typically, secondary injury cascades are thought to resolve within 1- to 3-months after a TBI of mild-to-moderate severity (Carroll et al., 2004; Kwok et al., 2008; Losoi et al., 2016). However, increasing literature has demonstrated that symptoms can persist for months to years following TBI, which can impact quality of life and ability to return to everyday activities (Carroll et al., 2020; Nelson et al., 2019; van der Naalt et al., 1999). It is currently unclear why particular individuals are susceptible to poor behavioral and cognitive outcomes post-TBI, but it has been theorized to be due to differences in the underlying pathophysiology.

Inflammation of the brain, known as neuroinflammation, is a regularly reported feature following TBI in the clinic and laboratory which is mediated by the primary immune cells of the brain called microglia and supported by other glia such as astrocytes (Cao et al., 2012; Johnson et al., 2013; Xue et al., 2021). Microglia maintain brain homeostasis by performing house-keeping functions such as refining neural circuitry as well as surveying for pathogens and cellular debris (Li & Barres, 2018; Nimmerjahn et al., 2005; Tremblay et al., 2011). When microglia detect neuronal damage, such as that which occurs following a TBI, they produce inflammatory cytokines in order to recruit additional immune cells and clear debris via engulfment, also known as phagocytosis (Bachiller et al., 2018; Gehrmann et al., 1995; Kofler & Wiley, 2011). A shift from microglial homeostasis is referred to as microglial reactivity, which typically encompasses inflammatory and phagocytic functionality that is associated with morphological changes (Cao et al., 2012; Stratoulas et al., 2019). Homeostatic microglia have a small circular somata and thin, highly branched processes, whilst, when microglia become reactive, the cell body begins to swell and processes reduce in complexity (Cao et al., 2012; Ziebell et al., 2015). Microglial reactivity is typically a transient response lasting for days to weeks in order to return brain homeostasis (Cao et al., 2012; Li & Barres, 2018). However, immunohistochemical and magnetic resonance imaging (MRI) studies of human cerebral tissue have reported microglial reactivity months to years after a TBI, which may exacerbate neuronal injury and, hence, worsen functional outcomes (Chaban et al., 2020; Gentleman et al., 2004; Johnson et al., 2013; Ramlackhansingh et al., 2011).

A number of studies have investigated how microglia respond over time following a TBI in preclinical models (Cao et al., 2012; Lafrenaye et al., 2015; Loane et al., 2014; Madathil et al., 2018; Morrison et al., 2017; Ziebell et al., 2012). These studies suggest that

microglial pro- and anti-inflammation and phagocytosis is beneficial for tissue repair in the days post-injury (Cao et al., 2012; Lafrenaye et al., 2015; Loane et al., 2014; Madathil et al., 2018; Morrison et al., 2017; Ziebell et al., 2012). Conversely, microglial pro-inflammation and phagocytosis that is evident months to years after a TBI has been correlated with increasing neuronal damage and behavioral impairments (Boone et al., 2019; Loane et al., 2014; Ritzel et al., 2020; Saba et al., 2021). Regardless of these findings, a distinct pattern of microglial functions over time following a TBI is still not able to be identified. This could be because particular populations of individuals are more vulnerable to developing long-term inflammation after a TBI than others. The majority of previous clinical and experimental TBI research has been conducted in males as they are more likely to endure a TBI due to their participation in risk-taking behaviors, such as reckless driving (Gupte et al., 2019; Mushkudiani et al., 2007). However, females also sustain TBI through a variety of mechanisms, including sport and assault (Gupte et al., 2019). The increasing literature that includes female participants indicates that biological sex can impact TBI recovery, where females report more severe and prolonged symptoms compared with males (Gupte et al., 2019; Mikolić et al., 2021). Although the mechanisms that underlie biological sex differences in recovery following TBI are currently unknown, microglia have been demonstrated to exhibit biological sex differences in the developing, adult, and aged brain as well as following TBI (Doran et al., 2019; Guneykaya et al., 2018; Villa et al., 2018; Villapol et al., 2017; Yanguas-Casás, 2020). However, the findings from the current literature are contradictory, thus, the differences in microglial function in the healthy brain as well as across time post-TBI between males and females remains unclear.

The current study is the first, to our knowledge, that investigates the proteome of microglia across time after a TBI in both biological sexes. To do this, we isolated microglia from the adult mouse brain via fluorescence-activated cell sorting (FACS) at 3-, 7-, or 28-days following a moderate TBI to get an indication of the short-term and delayed microglial response. TBI was reproduced in the laboratory using the midline fluid percussion injury (mFPI) model that produces pathology similar to what we see in human cases after a global or diffuse brain injury with a lack of bruising or cavitation (Rowe, Griffiths, & Lifshitz, 2016). Identification of microglial pathways after a TBI and potential therapeutic targets may assist the development of more effective interventions that improve functional outcomes in individuals living with a TBI. We hypothesized that microglia become reactive in the short-term following TBI that persists up to 28 days post-injury but differs between biological sexes.

2 | MATERIALS AND METHODS

2.1 | Breeding and housing of mice

Mouse care, handling, and surgical procedures were conducted under the Australian Code for the care and use of animals for scientific purposes, 8th edition 2013, and the University of Tasmania's

animal ethics, #A17680, #A18226. Male and female heterozygous CX3CR1^{GFP} mice ($n = 48$; JAX stock #005582; Jung et al., 2000) for FACS and proteomics and C57BL/6J mice ($n = 24$) for immunohistochemistry were bred at the University of Tasmania's Cambridge Farm Facility and transported to the Medical Science Precinct animal facility at 10-weeks of age. Once arriving at the Medical Science Precinct animal facility, animals were acclimated prior to surgical procedures. Animals were housed in optimouse cages with ad libitum access to food and water and a maximum of five mice per cage in 12-h light/dark cycles. This work is reported according to the Animal Research: Reporting in vivo Experiments (ARRIVE) guidelines.

2.2 | Midline fluid percussion injury

Mice were either subjected to a moderate midline fluid percussion injury (mFPI) or left as an uninjured control (naïve) and did not experience any surgical procedures. At 12–16 weeks of age (females: 19.9–28.2 g; males: 25.0–34.9 g), before surgical procedures started, animals were allocated randomly into groups of either naïve, 3-, 7-, or 28-days post-injury ($n = 6$ per sex/group). The investigator conducting the surgery was blinded to the injury groups in order to avoid bias in surgery outcomes. Craniotomy and mFPI induction were conducted according to the previously published methods (Rowe, Griffiths, & Lifshitz, 2016). Briefly, mice were anesthetized using 5% isoflurane at 1 L/min with 100% oxygen for approximately 5 min. Buprenorphine (Temgesic, 0.1 mg/kg) analgesic was then administered via subcutaneous injection, followed by the fur being shaved from the scalp and an injection of local anesthetic (bupivacaine, 0.025 mg/kg). Animals were left for 20 min in the holding cage warmed on a heat pad to onboard analgesics and mitigate pain wind-up. Mice were re-anesthetized with isoflurane (5% at 1 L/min) and secured in a stereotaxic frame using the ear and bite bars on a heat pad which remained at 37°C for the duration of the surgery with 3% anesthesia at 0.3 L/min maintained via nose cone. Antiseptic betadine (Sanofi, Australia) was used to clean the surgical site, which was removed with 70% alcohol solution, and eyes were kept moist with ophthalmic ointment. Anesthesia was monitored via steadiness of breath, heart rate, and absence of reflex, including the tail pinch and pedal withdrawal reflex. A midline sagittal incision was made from between the eyes to just behind the ears in order to expose the skull. The fascia was removed delicately and a thin circular disc was shaved from weed trimmer line and secured to the skull along the sagittal suture, halfway between bregma and lambda. The circular disc was used as a guide for the 3 mm trephine attached to a micro hand-drill chuck which was used to perform a craniotomy by interchanging the direction of turning the trephine. Bone debris was washed away using cool artificial cerebrospinal fluid (aCSF) and once the edges of the craniotomy site were extremely thin, the brain was exposed by gently removing the bone flap without disturbing the underlying dura. An injury hub was placed on top of the craniotomy site and secured onto the skull with cyanoacrylate gel to create a seal between the hub and the skull. The exposed skull was covered with methyl methacrylate cement (dental acrylic), the

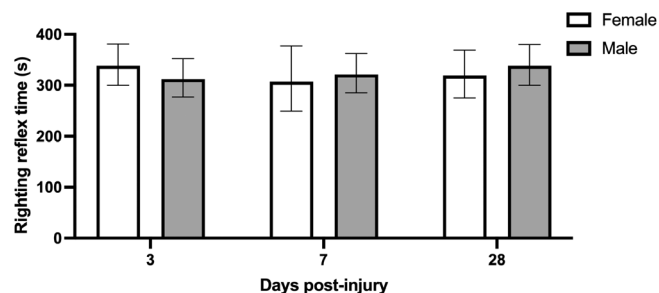


FIGURE 1 The duration of the righting reflex suppression in female (white) and male (gray) CX3CR1^{GFP} and C57BL/6J mice after a midline fluid percussion injury (mFPI) was used as a measure of injury severity with data represented as estimated marginal means \pm 95% confidence intervals (CI). Righting reflex times for each strain were combined for the purpose of this graph. Injury severity was relatively even across the 3-, 7-, and 28-days post-injury timepoints of both biological sexes ($\chi^2_2 = 1.5$; $p = .4715$), where the duration of the righting reflex suppression was between 5 and 10 min for all groups which is indicative of a moderate traumatic brain injury (TBI). [CX3CR1^{GFP} animals for proteomic analysis: $n = 6$ per group/sex, except for 7- ($n = 2$) and 28-days post-injury ($n = 4$) females. IHC analysis on C57BL/6J mice: $n = 6$ per group/sex].

hub was filled with aCSF to keep the brain moist, and mice were removed from anesthesia and the stereotaxic frame then placed in a pre-warmed holding cage until upright and alert.

Once mice had recovered for approximately 1 h, they were re-anesthetized using 5% isoflurane at 1 L/min and the injury hub was visually inspected for any obstructions or blood then filled with aCSF. The injury hub on the mouse was attached to the fluid percussion device to create a continuity of fluid between the injury hub and the fluid filled cylinder. As the animal regained the pedal reflex, the pendulum was released at an angle of 14° to produce a pressure pulse between 1.0 and 1.4 atm, resulting in an injury of moderate severity. The presence of apnea and seizures were recorded as well as the time taken for the mouse to regain the righting reflex which was used as a measure of injury severity, similar to previously published studies (Lifshitz et al., 2016; Rowe, Rumney, et al., 2016; Rowe, Ziebell, et al., 2016), and showed no difference between groups (Figure 1). Control animals were not exposed to anesthetics, surgery, or injury as such no righting reflex was recorded. Previous studies which use sham-injured or sham-surgery controls have reported righting reflexes of under 20 s (Green et al., 2021; Rowe et al., 2018; Rowe, Rumney, et al., 2016). This study incorporated naïve animals to minimize confounding variables similar to that of previously published works who also examined microglia following TBI (Doust et al., 2021; Hanscom et al., 2021; Witcher et al., 2021). Mice that had a duration of righting reflex suppression outside of the 5–10 min range were excluded from the study. Two female CX3CR1^{GFP} mice were excluded from this study as surgical failures due to righting times of 1 min 42 s and 1 min 36 s, respectively. Once the animal was upright, they were re-anesthetized, and the injury hub was removed to inspect the craniotomy site for signs of herniation, hematoma and integrity of the dura. After the wound was closed with sutures, the mice were placed in a

prewarmed holding cage for at least 1 h of recovery before being returned to the home cage and placed back in the colony. Naïve animals did not undergo any surgical procedures. Post-surgical evaluations were conducted twice daily for 3 days, then once a week until endpoint, to assess behavior, appearance, suture site and weight for any signs of pain or distress.

2.3 | Tissue collection and cell harvesting for proteomics

At 3-, 7-, or 28-days post-injury, or in a naïve state, CX3CR1^{GFP} animals were anesthetized with 5% isoflurane at 1 L/min and given a lethal dose of 115 mg/kg sodium pentobarbitone (Lethobarb, Troy Laboratories, Australia). Mice were transcardially perfused with 0.01 M phosphate buffered saline (PBS) and the brain was removed and homogenized through a 70 µm cell strainer (SPL life sciences, cat no. 93070) using a syringe plunger with 20 ml of 0.01 M PBS and 0.01 mg/ml of papain (Roche, cat no. 10108014001), 0.05% collagenase (Roche, cat no. 10269638001) and 0.025 U/ml DNase I (Roche, cat no. 10104159001) into a 50 ml falcon tube (Corning, USA). The 50-ml falcon tube was put into a bead bath at 38°C for 1 h, inverted every 15 min, then centrifuged at 20 RCF at 4°C for 5 min. The supernatant was removed and the pellet was triturated with 8 ml of 40% isotonic percoll, containing 1-part 1.5 M sodium chloride (NaCl) and 9-parts percoll (Sigma, cat no. E0414-1 L), in 0.01 M PBS. A 5 ml layer of 0.01 M PBS was gently placed on top of the percoll and centrifuged at 50 RCF at 4°C for 45 min with no brake. The supernatant was removed that contains myelin and the pellet, containing whole brain cell lysate, was triturated with 2 ml of 0.01 M PBS and strained through a 70 µm cell strainer with an extra 3 ml of 0.01 M PBS. The sample was then centrifuged at 20 RCF at 4°C for 5 min followed by the removal of the supernatant and the pellet triturated in 1 ml of 0.01 M PBS in preparation for FACS.

2.4 | Fluorescence-activated cell sorting of microglia

Microglia were isolated from whole brain cell lysate using the MoFlo AstriosEQ cell sorter (Beckman Coulter, USA), which was set up for operation according to the manufacturer's instructions. Briefly, the stream and lasers were aligned and PMT voltages were confirmed to be optimal using the automated quality control procedure whilst running cytometer set-up and tracking (CS&T) beads. Intellisort was enabled to set up sort parameters, including drop break-off, stream deflection, drop deposition and drop delay. The CyClone robotic arm was configured for sort collection and Summit software was used for obtaining, sorting, and interpreting flow cytometry data. The cell lysate was introduced into the Astrios at 60% pressure and microglia were identified as positive for enhanced green fluorescent protein (GFP) under the CX3CR1 promoter. The GFP-positive (GFP⁺) microglia were selected for enrichment sorting via gating (see Figure S1)

and collected in an Eppendorf tube with 100 µl 0.01 M PBS. The naïve samples contained ~250,000 GFP⁺ microglia per brain similarly to other published studies (Rangaraju et al., 2018), while samples from injured animals yielded ~350,000 GFP⁺ microglia per brain (see Figure S1). A limitation of isolating CX3CR1^{GFP+} cells is that we were unable to distinguish between microglia and peripheral macrophages. Previous studies have shown that majority of CX3CR1-expressing cells in the brain are microglia (reviewed in Wolf et al., 2013; Hughes et al., 2002). However, infiltration of peripheral myeloid cells occurs following mFPI, particularly in the acute phase (Witcher et al., 2020). By 3 days following mFPI the number of infiltrating macrophages (CD45-high/CD11b+ cells) subsides to sham levels (~5% of total CD11b+ cells; Witcher et al., 2020). In our study, 3 days post-injury was the earliest time point examined, therefore, the number of infiltrating macrophages would be consistent between naïve and injured samples and the changes in the proteome of CX3CR1^{GFP+} cells would likely be driven by microglia. Thus, in our study, we referred to the isolated CX3CR1^{GFP+} cells as microglia. Another limitation of this study is that we did not use a live/dead cell marker when isolating microglia via FACS, therefore, there is a possibility that the samples were contaminated with dead cells. Microglia samples isolated from naïve and injured animals were then centrifuged at 20 RCF at 4°C for 7 min. The supernatant was removed followed by the pellet being triturated in 100 µl of lysis buffer (7 M Urea, 2 M Thiourea, 20 mM Tris-HCl) and 1× protease inhibitor (Roche cOmplete mini-inhibitor, cat no. 11836153001) and stored at -80°C prior to protein extraction and digestion.

2.5 | Protein extraction and digestion

Microglia samples were sonicated three times, with 15 s in the sonicator and 5 s on ice, then kept at 4°C for 2 h. Protein concentration was determined by performing a Bicinchoninic Acid (BCA) assay as per manufacturer protocol (Pierce™ BCA protein assay kit, ThermoScientific) and adjusted to 50 µg/ml. Samples containing ~5 µg of protein were sequentially reduced and alkylated using standard methods, then digested at a 1:25 enzyme:protein ratio with proteomics grade trypsin/LysC (V5071; Promega, Madison, WI, USA) overnight at 37°C according to the SP3 method (Hughes et al., 2019). Following digestion, peptides were acidified with 2 µl of 1% TFA and then desalted using C18 ZipTips (Millipore, cat no. Z720070-96EA).

2.6 | High-performance liquid chromatography and data-independent acquisition mass spectrometry

Peptide samples were randomly allocated into two batches using Microsoft Excel version 16.54 and analyzed by data-independent acquisition (DIA) mass spectrometry (MS) using an Ultimate 3000 nano RSLC system coupled with a Q-Exactive HF mass spectrometer fitted with a nanospray Flex ion source (ThermoFisher Scientific, Waltham, MA, USA) and controlled using Xcalibur software



(v4.3; ThermoFisher Scientific). The investigator conducting the experiments was blinded to the injury groups to avoid introducing bias to the analysis. Approximately 1 μ g of each sample was separated using a 120 min gradient at a flow rate of 300 nl/min using a 250 mm \times 75 μ m PepMap 100 C18 analytical column, after preconcentration onto a 20 mm \times 75 μ m PepMap 100 C18 trapping column. Columns were held at 45°C. MS parameters used for data acquisition were: 2.0 kV spray voltage, S-lens RF level of 60 and heated capillary set to 250°C. MS1 spectra (390–1240 m/z) were acquired in profile mode at 120,000 resolution with an AGC target of 3e6. Sequential MS2 scans were acquired across 26 DIA \times 25 amu windows over the range of 397.5–1027.5 m/z , with 1 amu overlap between windows. MS2 spectra were acquired in centroid mode at 30,000 resolution using an AGC target of 1e6, maximum IT of 55 ms and normalized collision energy of 27.

2.7 | Protein identification, quantification, and normalization

DIA-MS raw files were processed using Spectronaut software (v14.8; Biognosys AB). A project-specific library was generated using the Pulsar search engine to search the DIA MS2 spectra against the *Mus musculus* UniProt reference proteome (comprising 44,456 entries, April 2017). Biognosys factory settings were used for both spectral library generation and DIA data extraction, with the exception that single-hit proteins were excluded. For library generation, search parameters allowed for N-terminal acetylation and methionine oxidation as variable modifications and cysteine carbamidomethylation as a fixed modification and up to two missed cleavages were permitted. Peptide, protein, and PSM thresholds set to 0.01. Mass tolerances were based on first pass calibration and extensive calibration for the calibration and main searches, respectively, with correction factors set to 1 at the MS1 and MS2 levels. Targeted searching of the library based on XIC extraction deployed dynamic retention time alignment with a correction factor of 1. Protein identification deployed a 1% q -value cut-off at precursor and protein levels, automatic generation of mutated peptide decoys based on 10% of the library and dynamic decoy limitation for protein identification. Protein label-free quantitation used the Quant 2.0 setting, based on MS2-level data using the intensity values for the Top3 peptides (stripped sequences) and cross-run normalization was based on median peptide intensity.

2.8 | Data filtering and statistical analysis

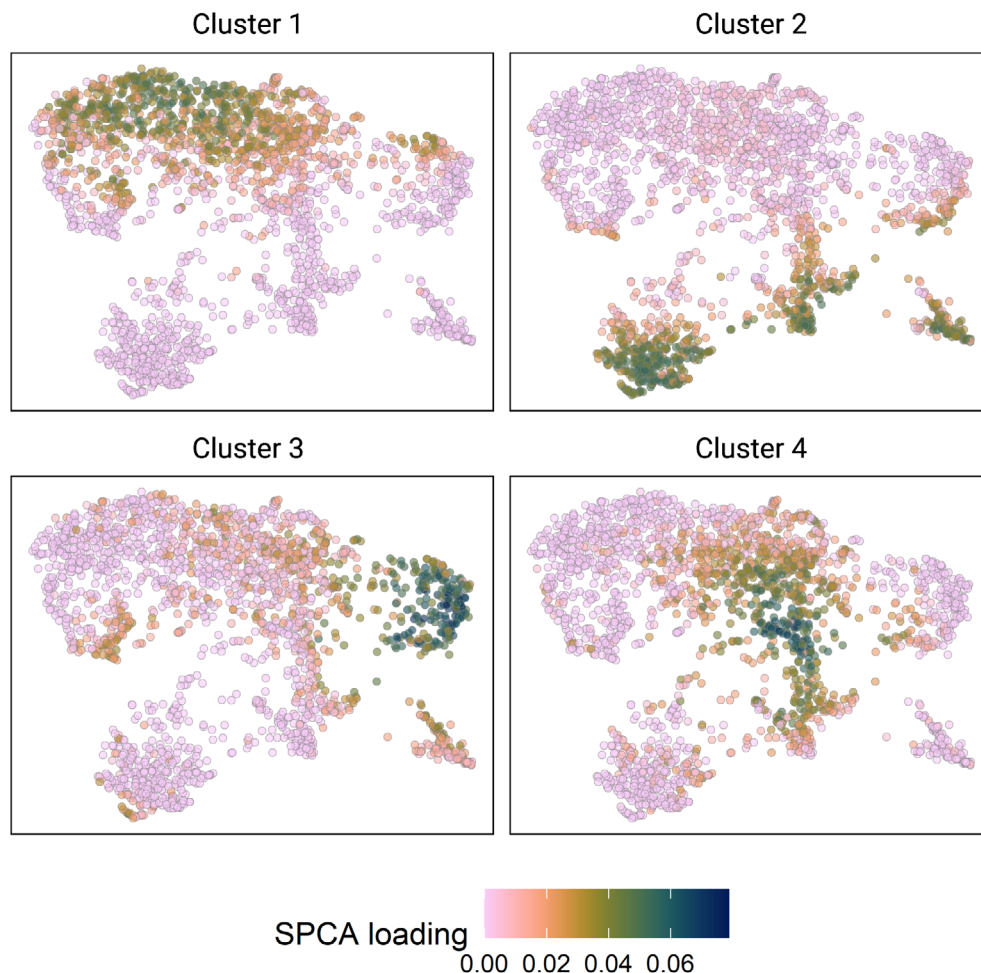
The Spectronaut protein output table was imported into Perseus software (Tyanova et al., 2016) and proteins identified in fewer than 50% of the samples were excluded from further analysis. Samples in which fewer than 1200 proteins were identified were also excluded from statistical analysis ($n = 2$ female mice at 7 days post-injury; $n = 2$ female mice at 28 days post-injury). Remaining missing values were imputed using default Perseus settings. The mass spectrometry proteomics data have been deposited to the ProteomeXchange Consortium

via the PRIDE (Perez-Riverol et al., 2022) partner repository with the dataset identifier PXD033628. Sparse principal component analysis (SPCA) was used to form a low-dimensional representation of the high-dimensional proteomics matrix. Classical principal component analysis (PCA) is known to be inconsistent when the number of dimensions (in this case proteins, p) is greater than the number of observations (in this case samples, n). SPCA resolves this issue by imposing a penalty on loadings, such that loadings that contribute little to the component can go to zero, and is consistent when $p \gg n$. We used the LASSO penalty (L_1 -norm) on the columns (p) and imposed a further constraint that non-zero loadings must be strictly positive. The penalty term was determined by 10-fold cross-validation following the method of (Witten et al., 2009) using the “PMA” package (Witten & Tibshirani, 2020) in R (R Core Team, 2021). The number of components was selected by trial and error, we stopped at i components when none of the explanatory variables were significantly associated with the $i + 1$ th principal component, since these were the variables of interest. The first four principal components explained 38.3% of variance, and there were 1295, 1519, 1234, and 1250 non-zero loadings, respectively, for each component. Each sparse principal component indicates a cluster of proteins with highly correlated protein abundance profiles across samples. Proteins do not necessarily load entirely on a single component, so clusters are not mutually exclusive. Principal component scores were computed for each sample for regression analysis, reducing the number of statistical comparisons with minimal information loss.

Univariate linear regression was used to estimate the association between explanatory variables time post-injury (in days), biological sex, and the score for each component. All regression models were adjusted to account for batch variation. We standardized each principal component by subtracting each score from the mean (for each component) and dividing by the standard deviation (SD) for each component, so that the effect of each explanatory variable could be interpreted on comparable scales across components. To estimate biological sex differences with time post-injury, we first fitted models with a time \times sex interaction term. If the time \times sex interaction term was not significant (F -statistic using type II sums of squares), we then fitted main effects models (additive terms only) to estimate average differences with time post-injury and biological sex differences averaged across time post-injury for each component. Results for the regression analyses are presented as standardized Beta coefficients with 95% confidence intervals (CI) on the SD scale for each component. We considered results significant at $p < .05$, and did not adjust for false discovery rate (reducing the number of comparisons by reducing the dimensionality of the data with a penalty prior to analysis, rather than post-hoc).

Uniform manifold approximation and projection (UMAP; McInnes et al., 2018) was used to reduce the p -dimensional matrix to two-dimensions to aid visualization of the SPCA results (Figure 2). The UMAP algorithm preserves local and global scale and is robust to nonlinearities, such that proteins which co-vary across samples are co-located in two-dimensional space. We shaded points using their corresponding SPCA loadings (unstandardized to preserve zeros),

FIGURE 2 Uniform Manifold Approximation and Projection (UMAP) of the total 2375 proteins identified within microglia where each dot represents a protein. Proteins with highly correlated protein abundance profiles across samples are co-located on the graph. We have shaded each protein using untransformed loadings from sparse principal components analysis (SPCA), each panel representing one of the four protein clusters ($n = 6$ per group/sex, except for 7- [$n = 2$ females] and 28-days [$n = 4$ females] post-injury).



arranged in a panel for each component. We used the “umap” (Konopka, 2020) and “ggplot2” (Wickham et al., 2016) packages to produce this figure. Code is provided in the Supporting Information, Data S1.

2.9 | Bioinformatics

Gene ontology (GO) and WikiPathway analysis was conducted using the STRING database (version 11.5; <https://string-db.org/>; Szklarczyk et al., 2018), an online bioinformatic resource. Protein lists included each sparse principal component which were analyzed using the mouse genome database. Over-represented ontologies and pathways were scored with p -values $< .05$, corrected for multiple testing using the Benjamin–Hochberg procedure, considered statistically significant.

2.10 | Tissue collection and preparation for immunohistochemistry

C57BL/6J mice were anesthetized with isoflurane (5%, 1 L/min) and given a terminal injection of 115 mg/kg sodium pentobarbitone (Lethobarb, Troy Laboratories, Australia) at 3- or 7-days post-injury, or in a naïve state. Once deeply anesthetized (absence of pedal

withdrawal reflex and deep breathing), animals were transcardially perfused using 4% paraformaldehyde (PFA) in 0.01 M PBS to clear the vasculature and fix the tissue. The cranium was removed and post-fixed in 4% PFA for 12 h, then moved to 0.02% sodium azide (NaN_3) in 0.01 M PBS and stored at 4°C prior to sectioning. The brain was removed from the skull in order to perform coronal sectioning at 40 μm using a Leica Microsystems VT1000E vibratome (USA) and the tissue was stored in a 24-well plate in PBS azide at 4°C preceding the conduction of immunohistochemistry.

2.11 | Triple-labeling of microglia with phagocytic and myelin markers

Three serial cortical sections (Bregma: 0.74, -1.64 , -2.75 mm), per brain, were washed three times in 0.01 M PBS for approximately 5 min per wash and placed in 100% methanol for 11 min at -20°C . Sections were washed again in 0.01 M PBS, then placed in 4% normal goat serum in 0.01 M PBS blocking solution for 60 min with agitation followed by incubation with rat anti-CD68 (1:500; BioRad, cat no. MCA1957GA) and rabbit anti-MBP (1:1000; Sigma, cat no. HPA049222) diluted in 1% block solution and 0.01 M PBS overnight at 4°C. All washes and incubations were conducted at room



temperature unless otherwise specified. The next day, the tissue sections were washed three times with 0.01 M PBS and incubated with goat anti-rat Alexa Fluor 488 (1:1000; Invitrogen, cat no. A-11006) and donkey anti-rabbit Alexa Fluor 594 (1:1000; Invitrogen, cat no. A-21207) diluted in blocking solution for 120 min shielded from light. After three 0.01 M PBS washes, sections were incubated with rabbit anti-Iba1 red fluorochrome(635)-conjugated antibody (1:250; WAKO, cat no. 013-26,471) for 60 min at room temperature followed by 7 days at 4°C. Sections were washed with 0.01 M PBS and mounted on glass slides (Dako, Denmark) and left to air dry for approximately 10 min before being coverslipped (Dako, Denmark) with PermaFluor aqueous mounting medium (Thermo Scientific, cat no. TA-030-FM). Immunohistochemistry experiments were conducted in one batch to avoid batch variation with the inclusion of a negative control (no primary antibody).

2.12 | Fluorescent microscopy, manual counts, and statistical analysis of microglia colocalization

Confocal microscopy was conducted using the Perkin-Elmer Ultra-VIEW VoX system, involving an inverted Ti Eclipse microscope (Nikon, Japan) with a CSU-X1 spinning disk confocal scanner (Yokogawa Electric Corporation, Japan). The plan apochromatic 40×/0.95 objective (Nikon, Japan) was used via the Volocity 6.3 software to capture z-stack images (1 image taken per 1 μm of optical thickness) in the corpus callosum and primary sensory barrel field (S1BF) of both hemispheres with excitation lasers/emission filters of wavelength 488/525, 561/615, and 633/738. Z-stacks were saved as OME.TIFF files for subsequent analysis as maximum intensity projection images that displays the multiple planes of the section in two dimensions. Microglial colocalization with phagocytic (CD68) and myelin (MBP) markers was conducted according to previously published methods (Doust et al., 2021). Briefly, a 1-mm² grid was placed across the image and all microglia were counted within each square, at random, using the cell counter tool, with a target of 100 microglia. The total number of microglia and the number of microglia colocalized with CD68 and MBP were summed for all six images per animal. The proportion of colocalized microglia per animal out of the total number of cells counted was determined by dividing the number of colocalized microglia by the total number of microglia then averaged across each group with 95% confidence intervals (CI). The binomial proportion of total microglia that were colocalized with CD68 and MBP was estimated using logistic regression in a generalized linear mixed effects model (McCulloch & Neuhaus, 2014). Random intercepts were fitted for each animal to account for clustering in the data and *p*-values were computed with Asymptotic Wald chi-squared tests using the “lme4” package (Bates et al., 2015) in the R statistical computing environment (R Core Team, 2021). The “emmeans” R package (Lenth et al., 2021) was used to compute estimated marginal means and post-hoc contrasts, with corrections for multiple comparisons using Tukey's method to appropriately control Type 1 errors.

3 | RESULTS

This study examined the proteins in microglia isolated from male and female CX3CR1^{GFP} mice at 3-, 7-, or 28-days after a mFPI as well as those in a naïve state to determine whether the microglial proteome changes with time post-injury between biological sexes. Of the 48 animals used for this study, results from 42 animals are presented here. Six females were excluded, two as surgical failures and four did not meet the requirements for protein detection threshold (<1200 proteins).

3.1 | Proteins isolated from adult microglia were divided into four clusters based on total abundance for bioinformatic analysis

For the initial protein analysis, 2375 proteins were detected using DIA-MS and changes in protein abundance were determined using sparse principal component analysis (SPCA). Similar to previously published literature (de la Fuente et al., 2020; Martin et al., 2020), SPCA was used to group proteins that may or may not be functionally related to one another into clusters based on protein abundance profiles. SPCA revealed four clusters of proteins that had distinct protein abundance profiles (Figure 2). The first three protein clusters identify the temporal profile of microglia across time post-injury (Figure 3). There were 1295 proteins (cluster 1) with significantly reduced protein abundance ($p = .003$) and 1519 proteins (cluster 2) with significantly increased protein abundance ($p = .002$) in microglia isolated from mice at 28 days following mFPI compared with naïve controls (see Table 1; Figure 3). There were 1234 proteins (cluster 3) with significantly reduced protein abundance at 3- ($p < .001$) and 7-days post-injury ($p = .014$) but returned to naïve levels by 28 days post-injury (see Table 1; Figure 3). These changes in protein abundance across time post-injury were evident to a similar extent in both males and females (sex × time interaction: $p = .266$, $p = .284$, $p = .823$, respectively). However, there were 1250 proteins (cluster 4) with significantly increased protein abundance in microglia isolated from male mice compared with those isolated from females ($p = .046$; see Table 1) which was evident in naïve animals as well as across time post-injury (sex × time interaction: $p = .322$; Figure 3). Proteins with loadings less than 0.02 in loading value were excluded from bioinformatic analysis. Therefore, bioinformatic analysis included 739, 579, 493, and 643 proteins, respectively, for each of the four clusters of proteins where proteins were grouped based on protein abundance profiles.

3.2 | The abundance of myelin and synapse “debris” and phagocytic proteins was decreased in microglia at 3- and 7-days post-injury regardless of biological sex

Using STRING gene ontology (GO) analysis, proteins with a significant reduction in abundance in microglia isolated from male and female

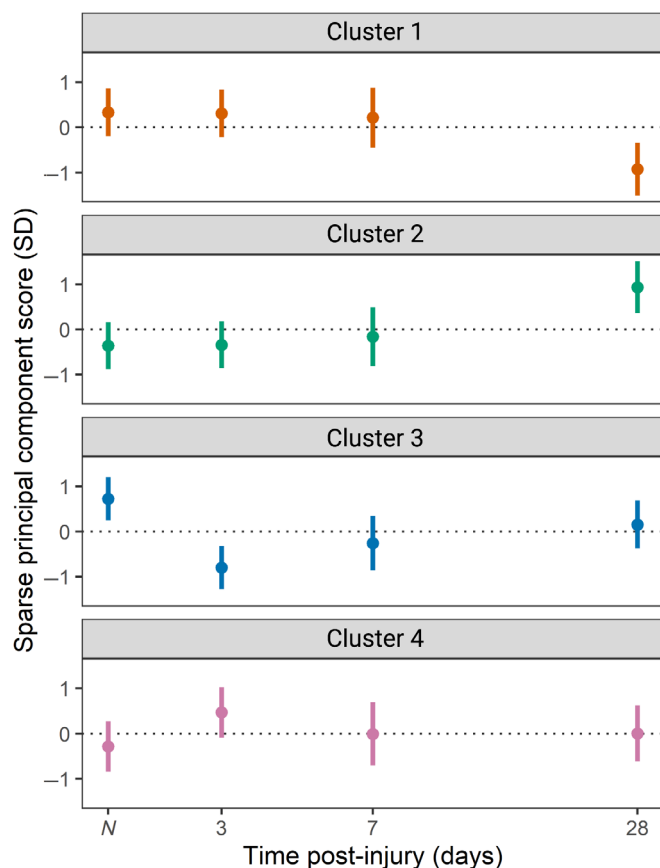


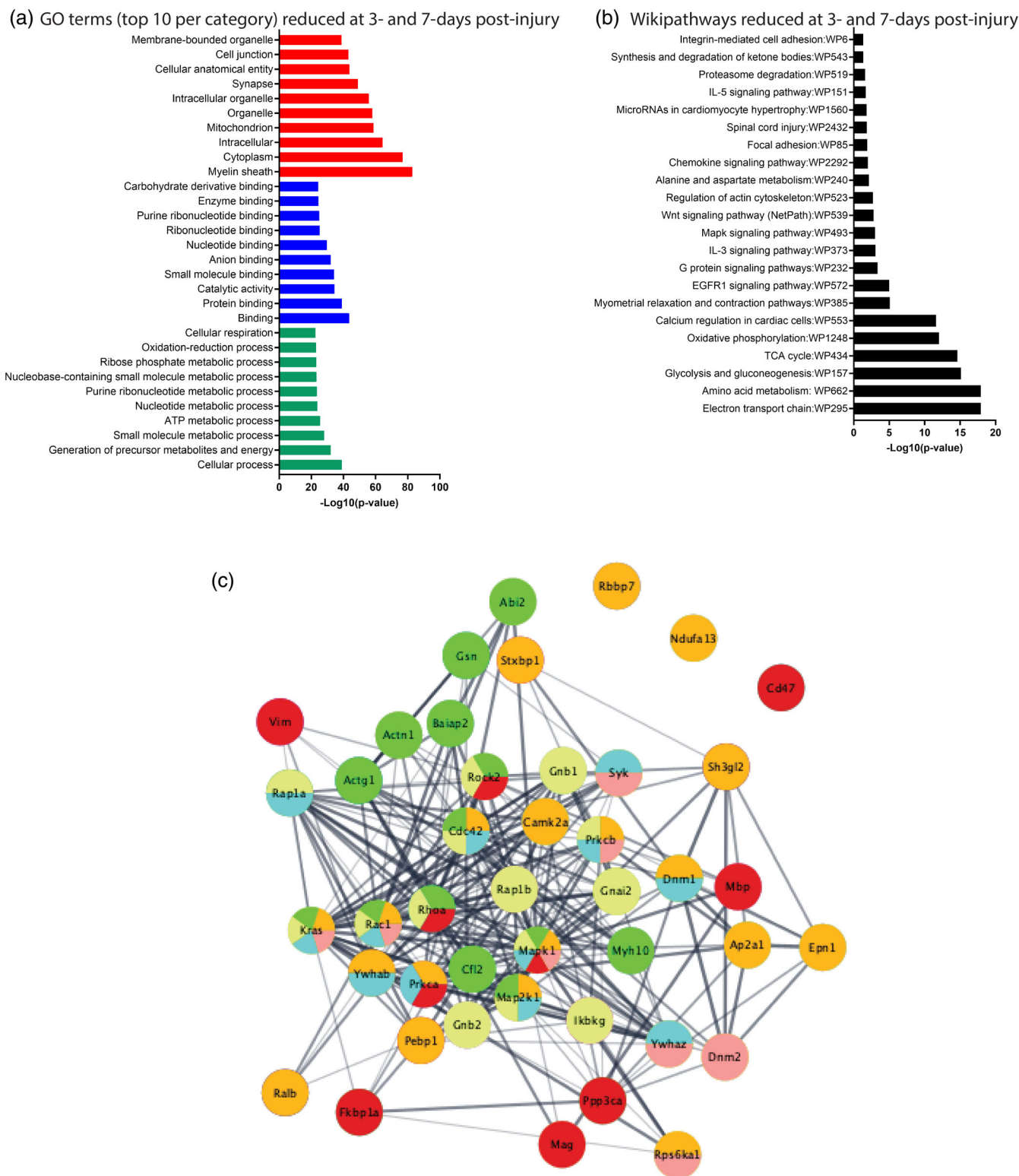
FIGURE 3 Sparse principal component scores indicating the magnitude and direction of changes in protein abundance for each of the four protein clusters across time post-injury (days), mean-centered and standardized to 1 unit SD. The sparse principal component scores for the first cluster of proteins were significantly decreased from naïve levels at 28 days post-injury, whilst the sparse principal component scores for the second cluster of proteins were increased at 28 days post-injury. The sparse principal component scores for the third cluster of proteins were significantly decreased at 3- and 7-days post-injury but returned to naïve levels by 28 days post-injury. There were no significant differences in sparse principal component scores for the fourth cluster of proteins across time post-injury. Estimated means and 95% confidence intervals are shown on unit standard deviation scale ($n = 6$ per group/sex, except for 7- [$n = 2$ females] and 28-days [$n = 4$ females] post-injury).

mice at 3- and 7-days following mFPI compared with microglia isolated from naïve animals were identified as being related to synapses and the myelin sheath (Figure 4a). Using *t*-test analysis to compare the sets of naïve animals with 3 days post-TBI ($FDR < 0.05$), we identified 50 significant proteins associated with the term myelin sheath. Representing the data for this set using a heat map demonstrated near-perfect clustering of the samples according to treatment, and confirmed the overall lower abundance levels for these proteins in samples collected from animals at 3 days post-injury (Figure S2). STRING Wikipathway analysis also revealed that proteins with reduced abundance at 3- and 7-days post-injury were involved with phagocytosis of neuronal debris ("regulation of the actin cytoskeleton: WP523", "spinal cord injury pathway:WP2432"; Figure 4b). The

TABLE 1 Sparse principal component (SPC) scores with time post-injury, compared with naïve levels, and between biological sexes (predictors)

Predictors	SPC 1			SPC 2			SPC 3			SPC 4		
	Std. Beta	Standardized CI	<i>p</i>	Std. Beta	Standardized CI	<i>p</i>	Std. Beta	Standardized CI	<i>p</i>	Std. Beta	Standardized CI	<i>p</i>
(Intercept)	0.33	-0.20 to 0.85	.247	-0.35	-0.87 to 0.17	.235	0.76	0.28 to 1.24	.003	-0.34	-0.89 to 0.22	.038
Time (3 days)	-0.02	-0.77 to 0.72	.949	0.02	-0.71 to 0.75	.96	-1.52	-2.20 to -0.84	<.001	0.75	-0.03 to 1.54	.06
Time (7 days)	-0.12	-0.96 to 0.72	.778	0.2	-0.63 to 1.03	.629	-0.98	-1.75 to -0.21	.014	0.28	-0.62 to 1.17	.533
Time (28 days)	-1.25	-2.04 to -0.47	.003	1.29	0.52 to 2.06	.002	-0.57	-1.28 to 0.15	.115	0.29	-0.54 to 1.12	.486
Sex (male)	0.08	-0.21 to 0.37	.595	-0.1	-0.39 to 0.18	.474	-0.25	-0.51 to 0.02	.064	0.31	0.01 to 0.62	.046
Batch	-0.14	-0.42 to 0.15	.344	0.14	-0.14 to 0.42	.328	0.01	-0.25 to 0.27	.925	0.16	-0.14 to 0.46	.288
Observations	42			42			42			42		
$R^2/R^2_{\text{adjusted}}$	0.293/0.195			0.313/0.218			0.413/0.331			0.209/0.099		

Note: Standardized beta coefficients (unit standard deviation scale) and their 95% CI are shown. Bold *p*-values indicate that the coefficients are statistically significant ($p < 0.05$).



proteins related to the “regulation of the actin cytoskeleton:WP523” are known to be involved with the formation phagosomes during phagocytosis (Mao & Finnemann, 2015). Additionally, proteins related to the “spinal cord injury pathway:WP2432” include myelin proteins (Mbp, Mag; Figure 4b) and FK506 binding protein 1a (Fkbp1a) which is involved in Fc gamma R mediated phagocytosis, suggesting that the proteins related to the “spinal cord injury pathway:WP2432” are involved with myelin phagocytosis (Bohdanowicz & Fairn, 2011). Proteins with reduced abundance at 3- and 7-days post-injury were also related to proliferation (“IL-5 signaling pathway:WP151”, “IL-3 signaling pathway:WP373”, “EGFR1 signaling pathway:WP572”) and cell migration (“chemokine signaling pathway:WP2292”; Figure 4b). Proteins related to proliferation and cell migration were also involved with phagocytosis of neuronal debris (see Table S2 for a list of proteins; Figure 4c) indicating that the phagocytosis pathways were intermingled with other immune-related functions. Proteins with reduced abundance at 3- and 7-days post-injury were also involved with amino acid metabolism (“amino acid metabolism:WP662”) and glycolysis (“glycolysis and gluconeogenesis:WP157”) as well as oxidative phosphorylation (“oxidative phosphorylation:WP1248”, “electron transport chain:WP295”, “TCA cycle:WP434”; Figure 4b). These results suggest that amino acid metabolism, glycolysis and oxidative phosphorylation are associated with microglial phagocytic activity which is in line with previous literature that have extensively reported that microglia utilize oxidative phosphorylation when undertaking phagocytic functions (reviewed in Lauro & Limatola, 2020; Yang et al., 2021). However, glycolysis and amino acid metabolism is typically correlated with pro-inflammatory functions (Geric et al., 2019; reviewed in Lauro & Limatola, 2020; Yang et al., 2021). Our findings support the increasing research that suggests that phagocytic microglia adopt a mixed mode of metabolism (Wang et al., 2019). These data indicate that proteins involved with phagocytosis of myelin and synapses were reduced in microglia isolated from male and female mice at 3- and 7-days post-injury compared with naïve controls. As we hypothesize that myelin was being phagocytosed by microglia, immunohistochemistry (IHC) was used to examine spatial relationships between microglia and engulfment of myelin.

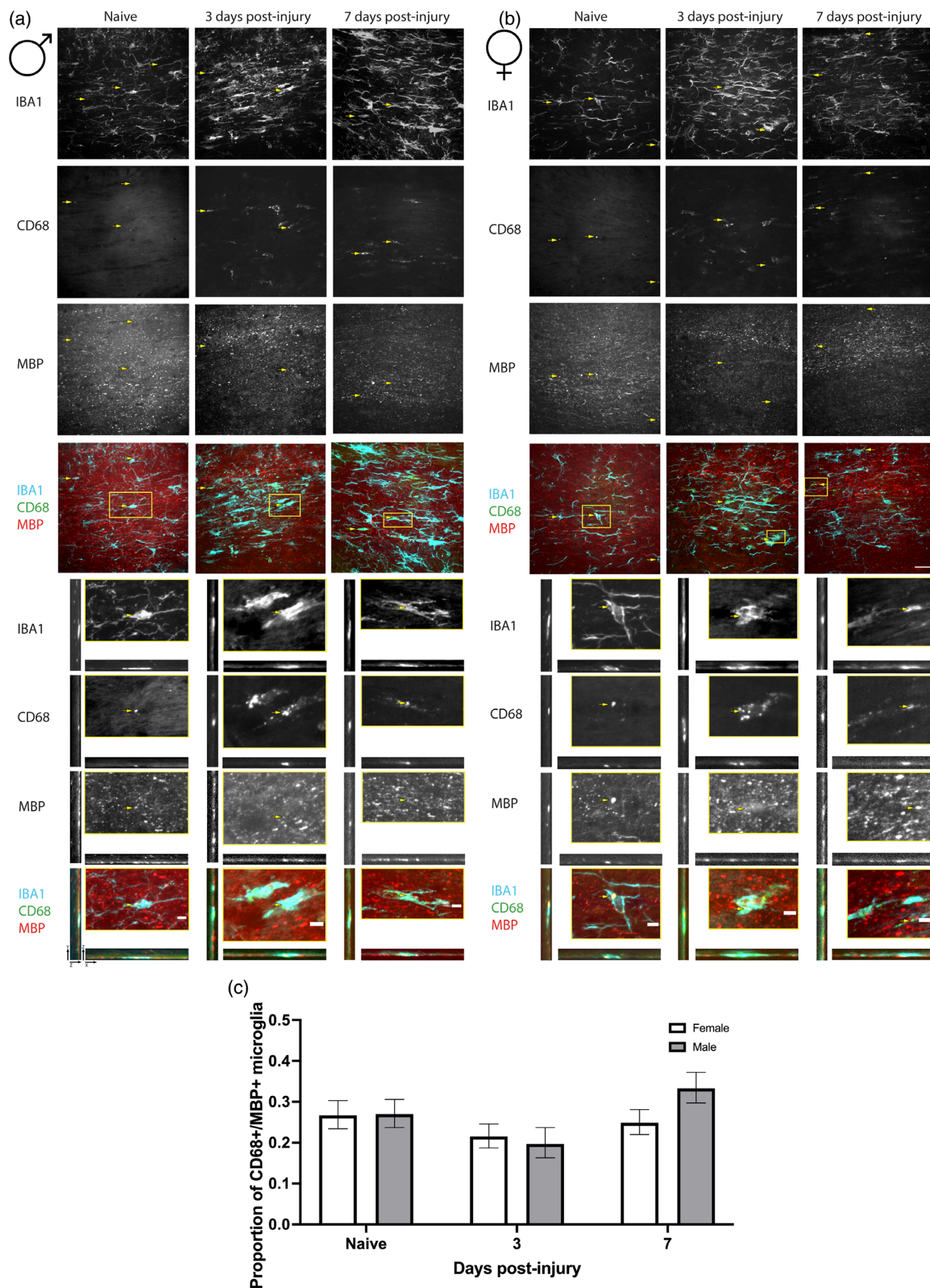
3.3 | Regional differences in microglial colocalization with CD68 and MBP at 3- and 7-days post-injury were evident in female but not male mice

Coronal sections from male and female C57BL/6J mice at 3- and 7-days post-injury and naïve animals were stained with ionizing calcium binding adaptor protein 1 (Iba1), cluster of differentiation 68 (CD68), and myelin basic protein (MBP). Iba1 was used to visualize microglia along with a surrogate marker of phagocytosis, CD68, and one of the key components of myelin, MBP, to investigate microglial phagocytosis of myelin following injury and between biological sexes. Microglia colocalization with CD68 and MBP was used in this study as a measure of microglial phagocytosis of myelin. Microglial phagocytosis of myelin was examined in the corpus callosum (CC; Figure 5)

and primary sensory barrel field (S1BF; Figure 6), where CD68 staining was most prevalent, and was reported in this study as the proportion of microglia colocalized with CD68 and MBP \pm 95% confidence intervals (CI). Regional differences in the proportion of CD68-positive/MBP-positive (CD68+/MBP+) microglia were observed across time post-injury and between biological sexes ($\chi^2 = 17.0$; $p < .0001$) (see Table S1 for estimated counts and their 95% CIs; depicted in Figures 5 and 6). In the CC, there was a significant reduction in the proportion of CD68+/MBP+ microglia at 3 days post-injury compared with naïve controls in both males ($p = .0062$; see Table 2; Figure 5) and females ($p = .0265$; see Table 2; Figure 5). There was a significant increase in the proportion of CD68+/MBP+ microglia in the CC of male mice at 7 days post-injury compared with sex-matched naïve controls ($p = .0154$; see Table 2; Figure 5) and at 3 days post-injury ($p < .0001$; see Table 2; Figure 5) but not in females. The proportion of CD68+/MBP+ microglia in the CC of male mice was also significantly greater than in females at 7 days post-injury ($p = .0005$; see Table 3; Figure 5). In the S1BF there was a significant decrease in the proportion of CD68+/MBP+ microglia at 3 days post-injury in males ($p = .0260$; see Table 2; Figure 6) whilst there was a significant increase in females ($p = .0044$; see Table 2; Figure 6) compared with sex-matched naïve controls. The proportion of CD68+/MBP+ microglia was also significantly greater in the S1BF of females compared with males at 3 days post-injury ($p < .0001$; see Table 3; Figure 6). At 7 days post-injury, there was a significant increase in the proportion of CD68+/MBP+ microglia in the S1BF of males compared with sex-matched naïve controls ($p = .0007$; see Table 2; Figure 6) and at 3 days post-injury ($p < .0001$; see Table 2; Figure 6). However, there was a significant reduction in the proportion of CD68+/MBP+ microglia in the S1BF of females at 7 days post-injury compared with sex-matched naïve controls ($p = .0132$; see Table 2; Figure 6) and at 3 days post-injury ($p < .0001$; see Table 2; Figure 6). The proportion of CD68+/MBP+ microglia was also significantly greater in the S1BF of males compared with female mice at 7 days post-injury ($p = .0001$; see Table 3; Figure 6). These results suggest that male mice exhibit a reduction in microglial phagocytosis of myelin at 3 days post-injury in both the CC and S1BF that becomes increased at 7 days post-injury above naïve levels. Female mice also experience a reduction in microglial phagocytosis of myelin at 3 days post-injury in the CC that returns to naïve levels by 7 days post-injury. However, in the S1BF, female mice exhibit an increase in microglial phagocytosis at 3 days post-injury which becomes reduced below naïve levels at 7 days post-injury. Therefore, regional differences in microglial phagocytosis of myelin at 3- and 7-days post-injury was dependent upon biological sex.

3.4 | The abundance of pro-inflammatory proteins was decreased and the abundance of anti-inflammatory proteins was increased in microglia at 28 days post-injury regardless of biological sex

Using STRING gene ontology (GO) analysis, proteins with a significant reduction in abundance in microglia isolated from male and female

**FIGURE 5** Legend on next page.

mice at 28 days following mFPI compared with microglia isolated from naïve animals were related to metabolic processes (Figure 7a). STRING Wikipathway analysis revealed that proteins with reduced abundance at 28 days post-injury were involved with pro-inflammation via the tumor necrosis factor alpha (TNF- α) nuclear factor kappa beta (NF- κ B) signaling pathway ("TNF- α NF- κ B signaling pathway:WP246") along with protein ("proteasome degradation:WP519") and mRNA metabolism ("mRNA processing:WP310"; Figure 7b). Proteins with reduced abundance at 28 days post-injury were also involved with proliferation ("IL-2 signaling pathway:WP450", "IL-3 signaling pathway:WP373" and "EGFR1 signaling pathway:WP572") and purine metabolism ("purine metabolism:WP2185") that was determined via Wikipathway analysis (Figure 7b). ATP is a type of purine that is released by damaged neurons to trigger the migration of microglia to the injury site and the metabolism of ATP by microglia promotes phagocytic and pro-inflammatory functions (Jassam et al., 2017). Furthermore, proteins with reduced abundance at 28 days post-injury were involved with amino acid metabolism ("amino acid metabolism:WP662"), fatty acid oxidation ("fatty acid beta-oxidation:WP1269", "mitochondrial fatty acid beta-oxidation:WP401") and oxidative phosphorylation ("oxidative phosphorylation:WP1248", "electron transport chain:WP295", "TCA cycle:WP454"; Figure 7b). These results suggest that amino acid metabolism, fatty acid oxidation and oxidative phosphorylation are associated with microglial pro-inflammation which is in line with previous literature that amino acid metabolism is utilized during pro-inflammatory functions (Geric et al., 2019). However, fatty acid oxidation is typically used by homeostatic and anti-inflammatory microglia to fuel house-keeping functions and tissue remodeling (Yang et al., 2021). Studies in macrophages have shown that fatty acid oxidation was important for the release of pro-inflammatory cytokines such as IL-1 β and IL-18 (Moon et al., 2016). These findings could have implications for microglial metabolic programming in relation to pro-inflammatory functions. Our findings indicate that there was a reduction in abundance of pro-inflammatory proteins in microglia isolated from male and female mice at 28 days post-injury.

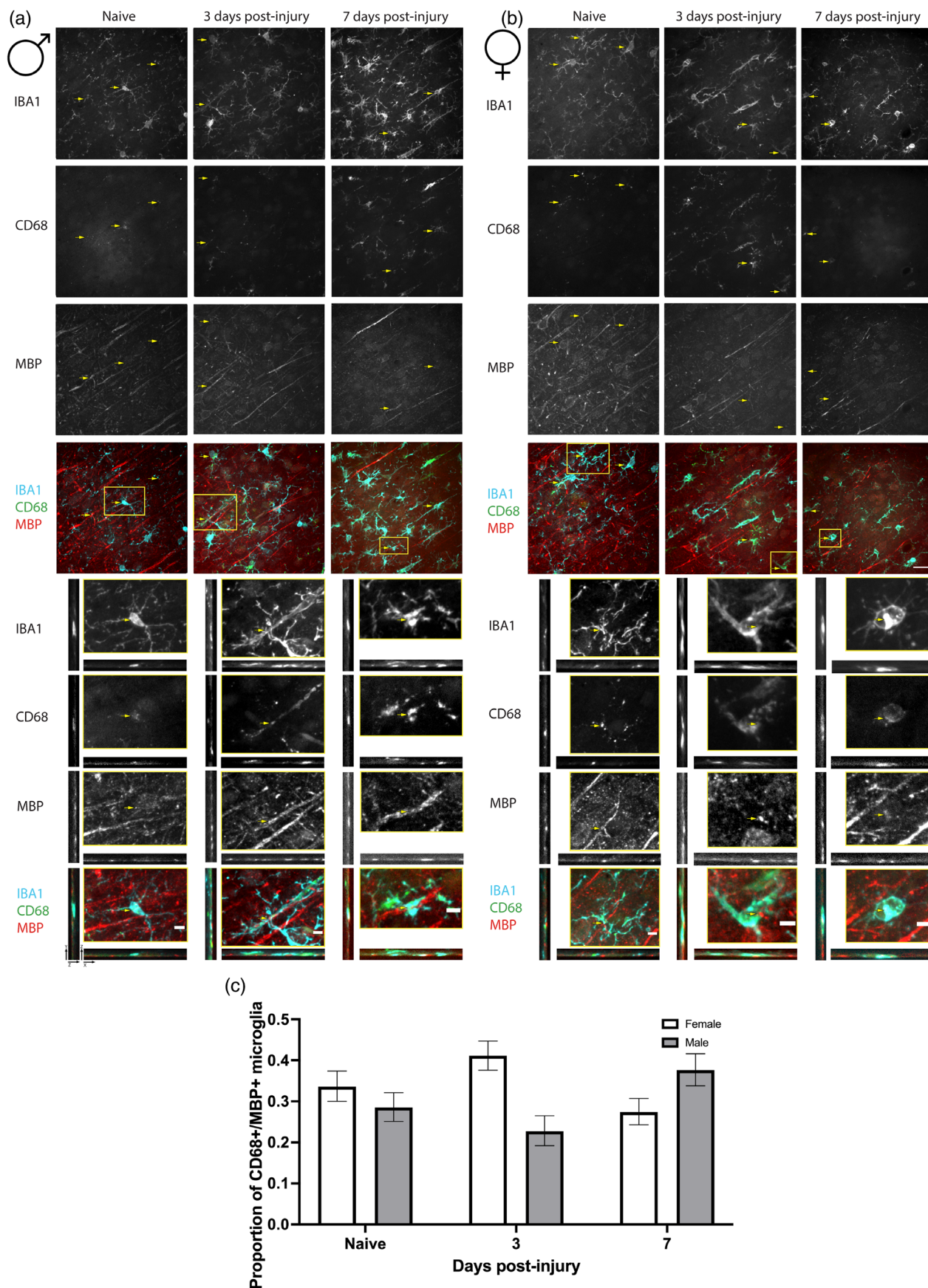
STRING gene ontology (GO) analysis also determined that proteins with a significant increase in abundance in microglia isolated from male and female mice at 28 days following mFPI compared with microglia isolated from naïve animals were related to gene expression and mRNA processing (Figure 7c). Additionally, STRING Wikipathway analysis revealed that proteins with an increased abundance at 28 days post-injury were involved with pluripotency ("PluriNetWork: mechanisms associated with pluripotency:WP1763") and protein ("cytoplasmic ribosomal proteins:WP163") and mRNA metabolism

("mRNA processing:WP310") (Figure 7d). Proteins with an increased abundance at 28 days post-injury were also related to TNF- α NF- κ B signaling ("TNF- α NF- κ B signaling pathway:WP246") which encompassed the A-kinase anchoring protein 8 (Akap8; see Table S3 for a list of proteins; Figure 7e). Akap8, also known as Akap95, is a protein that modulates toll-like receptor signaling and inhibits TNF- α NF- κ B-mediated pro-inflammation (Wall et al., 2009). TNF- α NF- κ B signaling proteins with an increased abundance were also distinct from TNF- α NF- κ B signaling proteins with reduced abundance (see Table S3 for a list of proteins; Figure 7e), indicating that proteins with an increased abundance and proteins with a reduced abundance at 28 days post-injury are involved with different TNF- α NF- κ B signaling cascades. Therefore, microglial proteins with an increased abundance at 28 days post-injury were involved with anti-inflammatory functions via TNF- α NF- κ B signaling. Proteins with an increased abundance at 28 days post-injury were also related to Wikipathways involved with oxidative phosphorylation ("electron transport chain:WP295"; Figure 8b). These results indicate that oxidative phosphorylation is associated with microglial anti-inflammatory function which is in line with previous literature (Holland et al., 2018; Yang et al., 2021). These results suggest that there was an increased abundance of anti-inflammatory proteins in microglia isolated from male and female mice at 28 days post-injury compared with naïves. Therefore, this data indicates that microglial pro-inflammation was reduced at 28 days post-injury whilst anti-inflammatory function was increased.

3.5 | Microglia isolated from male mice had increased abundance of pro-inflammatory, phagocytic, insulin signaling and estrogen signaling proteins compared with female mice

Using STRING gene ontology (GO) analysis, proteins with an increased abundance in microglia isolated from naïve and injured male mice compared with microglia isolated from naïve and injured females were related to cellular and metabolic processes (Figure 8a). Proteins with an increased abundance in naïve and injured males were identified via Wikipathways to be involved with pro-inflammation ("TNF- α NF- κ B signaling pathway:WP246", "IL-6 signaling pathway:WP387"), proliferation ("IL-2 signaling pathway:WP450", "IL-3 signaling pathway:WP373", "IL-5 signaling pathway:WP151", "IL-7 signaling pathway:WP297", "IL-9 signaling pathway:WP10", "EGFR1 signaling pathway:WP572"), cell migration ("chemokines signaling pathway:WP2292", "purine metabolism:WP2185") and phagocytosis ("regulation of actin cytoskeleton:WP523", "microglia

FIGURE 5 Example images of microglia colocalized with CD68 and MBP (indicated with yellow arrows) in the corpus callosum (CC) of male and female mice in a naïve state or at 3- or 7-days post-injury (a; scale bar = 25 μ m, inset = 5 μ m). Microglial colocalization with CD68 and MBP was quantified in the CC of both males (gray) and females (white) and expressed as the proportion of CD68+/MBP+ microglia (mean \pm 95%CI; b). There was a significant reduction in the proportion of CD68+/MBP+ microglia at 3 days post-injury in both males and females compared with sex-matched naïve controls (see Table 2). At 7 days post-injury, there was a significant increase in the proportion of CD68+/MBP+ microglia in males compared with sex-matched naïve controls and at 3 days post-injury, which did not occur in females (see Table 2). The proportion of CD68+/MBP+ microglia was also significantly greater in males compared with females at 7 days post-injury (see Table 3) (n = 6 per group/sex).

**FIGURE 6** Legend on next page.

pathogen phagocytosis pathway:WP3626"; Figure 8b). Proteins with an increased abundance in naïve and injured males were also involved with tyrosine kinase-binding protein (Tyrobp) signaling ("Tyrobp causal network in microglia:WP3625") identified via Wikipathway analysis (Figure 8b). Tyrobp is also known as DAP12 and is reported to be involved with proliferative and phagocytic functions in addition to being linked to the pathogenesis of Alzheimer's disease (AD) (Haure-Mirande et al., 2019; Yao et al., 2019). Additionally, proteins with an increased abundance in naïve and injured males were involved with serotonin signaling ("serotonin and anxiety:WP2141";

Figure 8b) which has been previously reported to enhance microglial migration to ATP, but, conversely, attenuates phagocytosis (Krabbe et al., 2012; reviewed in D'Andrea et al., 2020). Proteins with an increased abundance in naïve and injured males were also related to oxidative stress ("oxidative stress and redox pathway:WP4466; Figure 8b) which has been extensively reported to be triggered by pro-inflammation (reviewed in Lushchak et al., 2021). Therefore, microglia isolated from naïve and injured male mice exhibited an increase in abundance of pro-inflammatory and phagocytic proteins which involved Tyrobp and serotonin signaling in addition to oxidative

TABLE 2 Colocalized microglia post-hoc contrasts across time post-injury, separated by region and biological sex, using Tukey's procedure

Contrast: injury (Tukey)	Region	Sex	Co-efficient estimate	Lower 95% CI	Upper 95% CI	p-Values
N vs. 3DPI	CC	F	0.2825	0.0330	0.5321	.0265
N vs. 7DPI	CC	F	0.0915	-0.1471	0.3302	.4522
3DPI vs. 7DPI	CC	F	-0.1910	-0.4298	-0.0478	.1169
N vs. 3DPI	S1BF	F	-0.3231	-0.5456	-0.1007	.0044
N vs. 7DPI	S1BF	F	0.2937	0.0614	0.5260	.0132
3DPI vs. 7DPI	S1BF	F	0.6169	0.3967	0.8371	<.0001
N vs. 3DPI	CC	M	0.4098	0.1166	0.7031	.0062
N vs. 7DPI	CC	M	-0.3015	-0.5454	-0.0576	.0154
3DPI vs. 7DPI	CC	M	-0.7113	-0.9991	-0.4236	<.0001
N vs. 3DPI	S1BF	M	0.3073	0.0368	0.5778	.0260
N vs. 7DPI	S1BF	M	-0.4148	-0.6554	-0.1742	.0007
3DPI vs. 7DPI	S1BF	M	-0.7221	-0.9896	-0.4546	<.0001

Note: Co-efficient estimates and their 95% CI are shown. Bold indicates coefficients are statistically significant ($p < .05$).

TABLE 3 Colocalized microglia post-hoc contrasts between males and females, separated by region and injury status, using Tukey's procedure

Contrast: sex (Tukey)	Region	Injury	Co-efficient estimate	Lower 95% CI	Upper 95% CI	p-Values
F vs. M	CC	N	-0.0173	-0.267369	0.233	.8924
F vs. M	S1BF	N	0.2384	-0.000837	0.478	.0508
F vs. M	CC	3DPI	0.1100	-0.182805	0.403	.4615
F vs. M	S1BF	3DPI	0.8689	0.613092	1.125	<.0001
F vs. M	CC	7DPI	-0.4103	-0.642765	-0.178	.0005
F vs. M	S1BF	7DPI	-0.4701	-0.703798	-0.236	.0001

Note: Co-efficient estimates and their 95% CI are shown. Bold indicates coefficients are statistically significant ($p < .05$).

FIGURE 6 Example images of microglia colocalized with CD68 and MBP (indicated with yellow arrows) in the primary sensory barrel field (S1BF) of male and female mice in a naïve state or at 3- or 7-days post-injury (a; scale bar = 25 μ m, inset = 5 μ m). Microglial colocalization with CD68 and MBP was quantified in the S1BF of both males (gray) and females (white) and expressed as the proportion of CD68+/MBP+ microglia (mean \pm 95%CI; b). There was a significant reduction in the proportion of CD68+/MBP+ microglia at 3 days post-injury in males compared with sex-matched naïve controls (see Table 2). Whilst females experienced a significant increase in the proportion of CD68+/MBP+ microglia at 3 days post-injury compared with sex-matched naïve controls (see Table 2). The proportion of CD68+/MBP+ microglia was also significantly greater in females compared with males at 3 days post-injury (see Table 3). At 7 days post-injury, there was a significant increase in the proportion of CD68+/MBP+ microglia in males compared with sex-matched naïve controls and at 3 days post-injury (see Table 2). However, females exhibited a significant reduction in the proportion of CD68+/MBP+ microglia at 7 days post-injury compared with sex-matched naïve controls and at 3 days post-injury (see Table 2). The proportion of CD68+/MBP+ microglia was also significantly greater in males compared with females at 7 days post-injury (see Table 3) ($n = 6$ per group/sex).

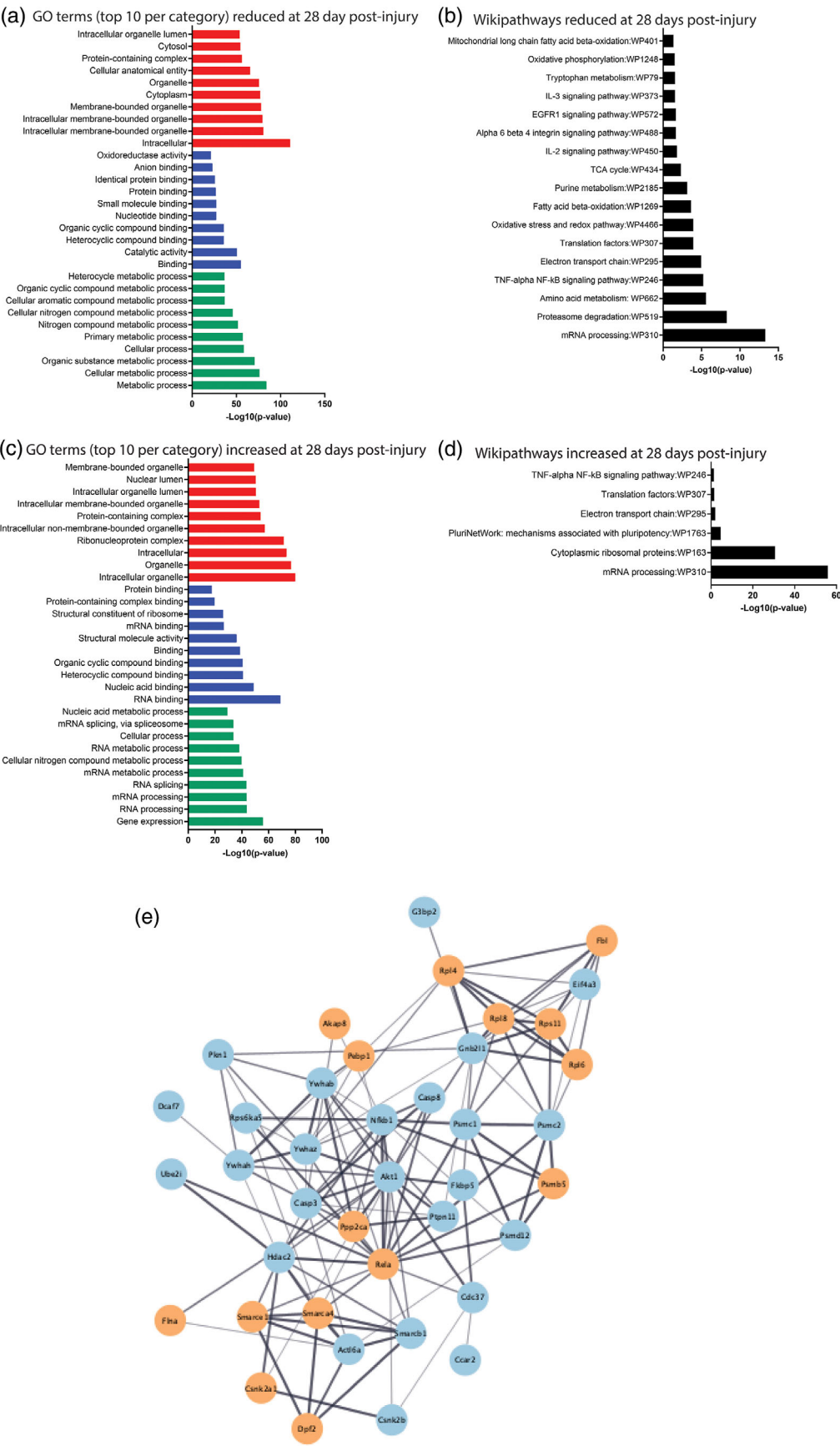


FIGURE 7 Legend on next page.

stress. Furthermore, proteins with an increased abundance in naïve and injured males were involved with amino acid metabolism (“amino acid metabolism:WP662”) and glycolysis (“pentose phosphate pathway:WP63”; Figure 8b). These results suggest that amino acid metabolism and glycolysis are associated with microglial pro-inflammation and phagocytosis which is in line with previous literature (Geric et al., 2019; Wang et al., 2019; reviewed in Lauro & Limatola, 2020). Proteins with an increased abundance in naïve and injured males were also involved with insulin (“insulin signaling:WP65”) and estrogen signaling (“estrogen signalling:WP1244”) that was determined via Wiki-pathway analysis (Figure 8b). Notably, The Akt1 protein was involved with pro-inflammation (“TNF-alpha NF-kB signaling pathway: WP246”), insulin (“insulin signaling:WP65”) and estrogen signaling (“estrogen signaling:WP1244”), suggesting that Akt1 may be involved in microglial biological sex differences of these pathways (see Table S4 for a list of proteins; Figure 8c). However, these pathways are extremely complex and our current study design cannot determine what is driving the changes in each pathway. This data indicates microglia isolated from naïve and injured male mice had an increase in pro-inflammatory, phagocytic and metabolic signaling proteins compared with microglia isolated from naïve and injured female mice.

4 | DISCUSSION

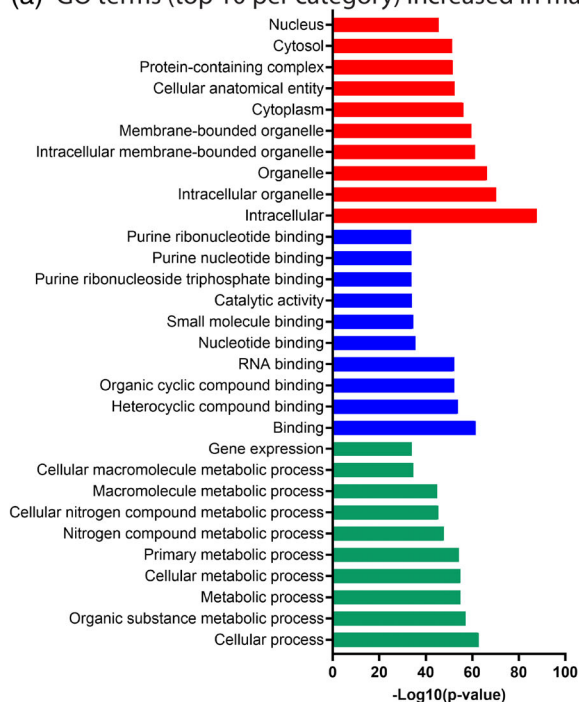
The microglial response, consisting of pro-inflammation and phagocytosis, is typically thought to peak in the days to weeks following TBI which is beneficial for tissue repair (Cao et al., 2012; Loane et al., 2014; Rowland et al., 2020; Smith et al., 2013). Microglia have also been reported to exhibit biological sex differences in the healthy brain as well as after a TBI which may impact TBI recovery (Doran et al., 2019; Guneykaya et al., 2018; Villa et al., 2018; Villapol et al., 2017; Yanguas-Casás, 2020). Therefore, this study sought to identify a distinct pattern of microglial functions across time after a TBI in both biological sexes. To do this, we examined the microglial proteome at 3-, 7-, and 28-days following a single diffuse TBI (mFPI) in male and female mice. The overall goal of this study was to provide a global analysis of microglial pathways that change across time following a TBI and between biological sexes. Mass spectrometry provides information about the relative abundances of each protein; however, the activity/functional capacity of each protein remains unknown. In addition to the identification of biological processes and pathways, our open-access dataset is available as a potential source of protein biomarkers and paves the way for further analysis in an independent cohort of animals including validation using orthogonal

techniques. To the best of our knowledge this is the first study to examine the proteome of isolated microglia after a TBI. Overall, the results from this study showed the abundance of myelin and synapse “debris” as well as phagocytic proteins was decreased in microglia at 3- and 7-days post-injury compared with naïve, with an increase in abundance of anti-inflammatory proteins at 28 days post-injury in both biological sexes. Microglia isolated from naïve and injured male mice also exhibited an increased abundance of pro-inflammation and phagocytic proteins as well as insulin and estrogen signaling proteins compared with those isolated from naïve and injured female mice.

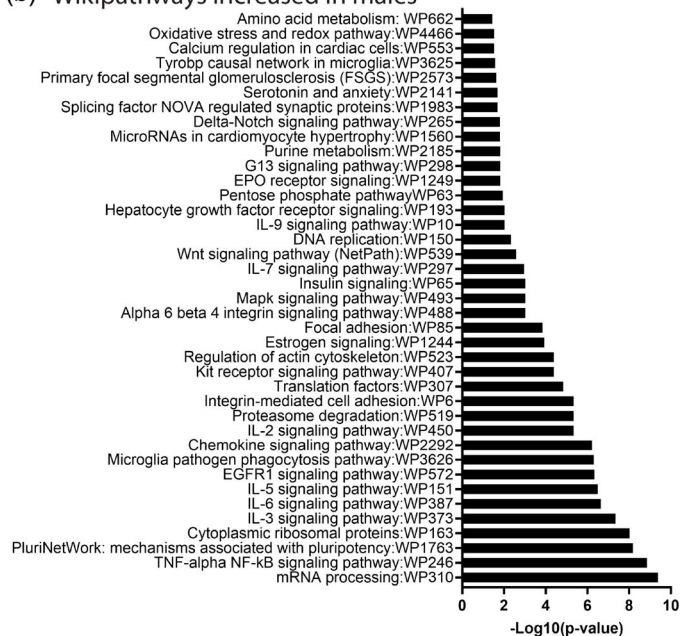
Neuronal debris is known to accumulate in the brain after a TBI and has been associated with the presentation of symptoms. Previous studies using male rodents have shown that a single diffuse TBI can induce neuron loss in the sensory cortex in addition to motor and neurological deficits in the days post-injury (Lifshitz & Lisembee, 2012; Rowe et al., 2019). Myelin damage in the corpus callosum has also been associated with cognitive dysfunction days to months after a TBI in male mice (Nonaka et al., 2021; Taib et al., 2017). It has been reported that microglia migrate to the injury site and phagocytose neuronal debris following injury. For example, in the minutes following a focal needle-stick injury in larval zebrafish, live confocal microscopy has directly shown microglial migration and phagocytosis of damaged neurons (Herzog et al., 2019). Furthermore, after a diffuse TBI (mFPI) in male rats, the amount of cluster of differentiation 68 (CD68) immunoreactivity, which is a surrogate marker of phagocytosis, was increased above naïve levels as early as 6 h post-injury in the neocortex, hippocampus and thalamus that remained elevated at 7-, 14-, and 28-days (Kelley et al., 2007). These studies demonstrate that microglia phagocytosis occurs early after a TBI and still remains evident at 28 days post-injury in specific regions of the brain. In our study, microglia isolated from male and female mice at 3- and 7-days post-injury exhibited a reduction in abundance of phagocytic proteins as well as myelin and synapse “debris” which returned to naïve levels by 28 days. It is possible that our proteomic data did not detect an increase in microglial proteins related to phagocytosis across time post-injury due to the global analysis conducted in this study which captured the average microglial function across the entire brain. Our immunohistochemical analysis allowed us to examine the spatial relationship in microglial phagocytosis of myelin across time post-injury and between biological sexes. We observed regional differences in the proportion of microglia colocalized with a CD68 and one of the key constituents of myelin (MBP) in females but not males. These findings suggest that subtle regional changes in microglial phagocytosis of neuronal elements occur across time post-injury and between biological sexes that were not able to be detected using a global

FIGURE 7 STRING gene ontology (GO; a) and WikiPathway (b) analysis of the 739 proteins with a significant reduction in abundance at 28 days post-injury in microglia isolated from both male and female mice. STRING gene ontology (GO; c) and WikiPathway (d) analysis of the 579 proteins with a significant increase in abundance at 28 days post-injury in microglia isolated from both male and female mice. GO analysis includes the top 10 GO terms per category; biological process (green), molecular function (blue) and cellular component (red). STRING protein interaction network (e) of the proteins reduced (blue) and increased (orange) at 28 days post-injury that were involved with TNF- α NF- κ B signaling (“TNF-alpha NF-kB signaling pathway:WP246”) ($n = 6$ males and $n = 4$ females at 28 days post-injury).

(a) GO terms (top 10 per category) increased in males



(b) Wikipathways increased in males



(c)

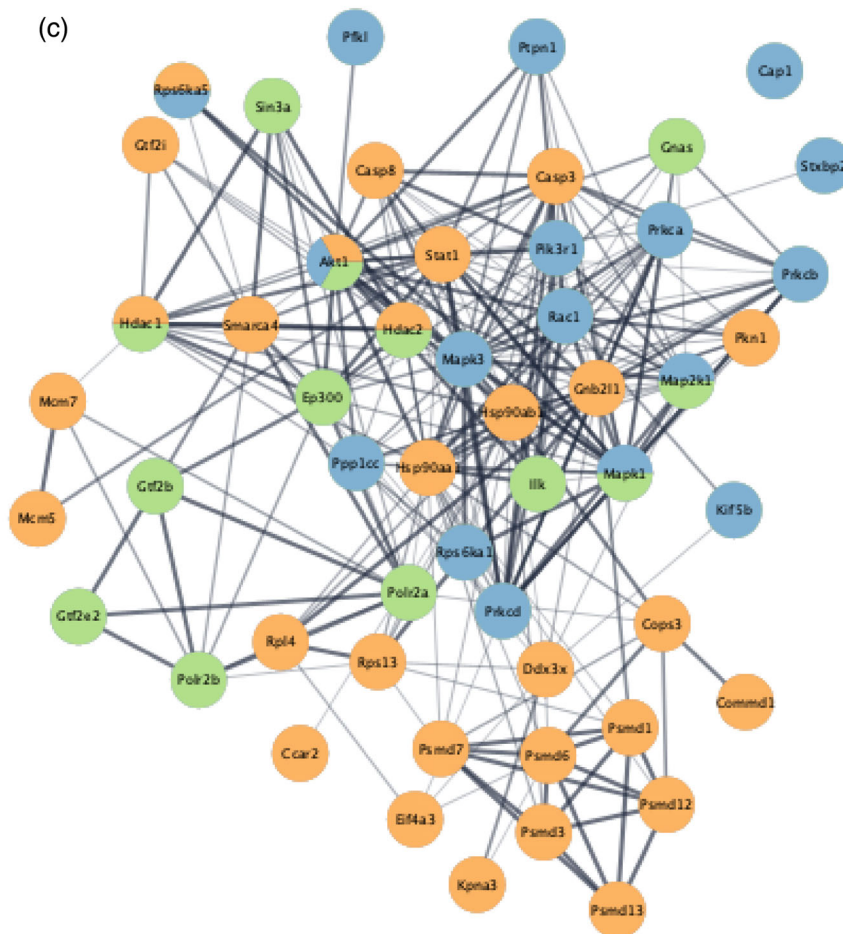


FIGURE 8 Legend on next page.

whole brain analysis. The consequence of microglia phagocytosis is unclear, however elevated microglial phagocytosis of neuronal elements 8 months after a focal TBI in male mice was correlated with poor motor, cognitive, and social outcomes (Ritzel et al., 2020). A limitation of this study was that we did not examine whether TBI-induced changes in microglial phagocytic proteins contributed to neuropathology or myelin damage post-injury or if there were differences between biological sexes.

Numerous studies have shown microglia participating in inflammatory functions after a TBI and our results do show a reduction in microglial pro-inflammatory proteins at 28 days post-injury along with an increase of anti-inflammatory proteins indicating that microglia are acting to promote tissue repair at 28 days after a TBI. There are conflicting reports about pro-inflammatory phenotypes with some studies in rodents showing microglial morphological changes along with an increase in pro-inflammatory mRNA, including MHCI, MHCII, IL-1 β , CD45, and translocator protein 18 kDa (TSPO), in the days post-injury in the cortex, hippocampus, and thalamus using both focal and diffuse TBI models (Cao et al., 2012; Madathil et al., 2018). Furthermore, a recent study also reported elevated pro-inflammatory mRNA expression in the cortex of male mice at 1-, 7-, and 30-days following mFPI identified via NanoString and single-cell sequencing (Witcher et al., 2021). However, other studies have shown that pro-inflammatory mRNA in the cortex and thalamus returned to naïve levels by 28 days after mFPI determined using real-time qPCR (Cao et al., 2012). Our study supports the notion that the pro-inflammatory function of microglia is not elevated above naïve levels at 28 days post-injury. However, in our study, pro-inflammatory protein levels were reduced below naïve levels at 28 days post-injury. The reason for these differences could be the discrepancies between transcription and translation or may relate to protein degeneration. The correlation between mRNA and protein levels are notoriously poor, due to mRNA post-translational processing (Koussounadis et al., 2015), and it is unclear how these data translate to protein levels and, thus, functional capacity. Additionally, an increase in microglial pro-inflammation after a TBI may also be dependent upon brain region. However, we did not examine pro-inflammatory profiles in situ for this current study. These changes in microglial phenotype may also be due to the continuum of inflammatory markers that microglia can express. For example, microglia can switch between pro- and anti-inflammatory markers as well as express a range of both simultaneously (Izzy et al., 2019; Kumar et al., 2016; Liu et al., 2021; Morganti et al., 2016). Others have demonstrated an extended shift toward a pro-inflammatory profile in the months to years post-TBI which has been correlated poor cognitive and behavioral outcomes (Boone et al., 2019; Johnson et al., 2013; Loane et al., 2014). A limitation of the

current study is the lack of chronic timepoints, however our data, in conjunction with previous literature, indicates peaks and troughs in microglial pro- and anti-inflammatory profiles across time after a TBI. The lack of differences in inflammatory proteins observed in this study during the acute phase post-injury might be due to the abundance of effector proteins being overlooked in this analysis. Inflammatory proteins are typically secreted from microglia to act upon other cells such as neurons and astrocytes (reviewed in Matejuk & Ransohoff, 2020; reviewed in Gao et al., 2013). Other proteomic studies post-TBI use whole brain homogenate which contains extracellular components such as effector proteins (Abu Hamdeh et al., 2018; Luo et al., 2021; Zhang et al., 2021). In this study, we isolated microglia from whole brain homogenate, thus, we cannot detect proteins that have been secreted from microglia. We cannot conclude that microglia have secreted inflammatory proteins into the extracellular space, but in this study these proteins were detected at naïve levels within microglia in the days following TBI.

A core aspect of our study was to examine if there were differences between males and females in the microglial response to TBI. A number of studies have reported that male rodents exhibit a greater inflammatory and phagocytic response in the short-term following TBI using immunohistochemistry and transcriptional profiling (Bromberg et al., 2020; Liu et al., 2021; Villapol et al., 2017). However, we found no biological sex differences in the microglial proteome across time post-injury suggesting that at the protein level the global microglial response is similar between males and females in the first 28 days post-injury. This is in line with previous literature that did not observe any significant differences in the expression of pro- or anti-inflammatory cytokines, production of reactive oxygen species (ROS) or microglial phagocytic activity at the protein level using flow cytometry up to 7 days following a controlled cortical impact (CCI) between male and female mice (Doran et al., 2019). Furthermore, flow cytometry and enzyme-linked immunosorbent assay (ELISA) analysis of microglial pro-inflammatory cytokines at the protein level up to 7 days post-CCI in male and female rats showed no biological sex differences (Scott et al., 2022). Conversely, Doran et al., 2019 identified an influx of peripheral myeloid cells and microglial proliferation at 1- and 3-days post-injury in male mice, which did not occur in females. Potentially this influx of peripheral cells drives behavioral changes following TBI, however, neither of these were examined in the current study. A recent study has shown that diffuse TBI (mFPI) induces a greater infiltration of peripheral immune cells compared with focal TBI (IFPI; Witcher et al., 2020). Therefore, biological sex differences in the inflammatory response following diffuse TBI may not be driven by microglia. Additional studies are required to better understand the

FIGURE 8 STRING gene ontology (GO; a) and WikiPathway (b) analysis of the 643 proteins with a significant increase in abundance in microglia isolated from naïve and injured male mice compared with those isolated from naïve and injured female mice. GO analysis includes the top 10 GO terms per category; biological process (green), molecular function (blue) and cellular component (red). STRING protein interaction network (c) of proteins increased in males involved with pro-inflammation (“TNF-alpha NF-kB signaling pathwayWP426”—orange) as well as insulin (“insulin signaling:WP65”—blue) and estrogen signaling (“estrogen signaling:WP1244”—Green) ($n = 6$ per group/sex, except for 7- [$n = 2$ females] and 28-days [$n = 4$ females] post-injury).



contributions of microglia and peripheral immune cells following TBI in relation to biological sex. In our study, we did identify an increased abundance of pro-inflammatory and phagocytic proteins in microglia isolated from naïve and injured male mice compared with those isolated from female mice. In line with previous literature, there was a greater amount of pro-inflammatory and phagocytic proteins in microglia isolated from male mice in a naïve state compared with females (Doran et al., 2019; Guneykaya et al., 2018; Villa et al., 2018). Following TBI, this pattern of protein expression remained. The pro-inflammatory and phagocytic proteins elevated in microglia isolated from naïve and injured male mice were distinct from those that changed across time post-injury. Therefore, pro-inflammatory and phagocytic pathways that are altered between biological sexes are different from those that change across time following TBI. Others have reported heightened pro-inflammatory and phagocytic profiles of microglia from a second insult after TBI, especially in relation to infection following TBI and repeated TBI (Fenn et al., 2014; Shitaka et al., 2011; reviewed in Witcher et al., 2015). However, a greater level of pro-inflammatory and phagocytic proteins in naïve males observed in this study did not produce an exaggerated microglial response following TBI. This may be partially explained by differences in injury model and techniques to assess microglial function (Sharma et al., 2021; Shitaka et al., 2011; Witcher et al., 2020).

Our study also highlighted differences in microglia insulin and estrogen signaling pathways between males and females in a naïve state and following TBI. Previously it has been reported that insulin metabolic signaling can promote pro-inflammatory and phagocytic pathways in microglia from male mice in vitro and in vivo (Brabazon et al., 2018; Haas et al., 2020; Spielman et al., 2015). Insulin secretion has also been shown in whole brain homogenate using mass spectrometry to increase acutely following severe CCI in male rats (Luo et al., 2021). This may have consequences for regulating metabolism after a TBI, especially given that endocrine dysfunction is a regularly reported feature following TBI (reviewed in Li & Sirko, 2018). The role of estrogen in the brain has been extensively reported to exhibit anti-inflammatory properties and promote cell survival and neuroplasticity under homeostatic and pathological conditions, such as after a TBI (Wang et al., 2021; Honig et al., 2021; reviewed in Kövesdi et al., 2020). However, estrogen synthesized from testosterone during development has been shown to induce microglial morphological changes and the production of pro-inflammatory cytokines, particularly prostaglandin E_2 (PGE_2) which is integral in the masculinization of the male brain (Lenz et al., 2013). A reduction in testosterone and an increase in estrogen production in young and older men has also been correlated with increased systemic pro-inflammatory cytokines (Bobjer et al., 2013; Maggio et al., 2009; Barud et al., 2010). Therefore, estrogen synthesized from testosterone may promote pro-inflammatory functionality of microglia in the adult male brain. However, these pathways are complex and our current study design cannot determine what is driving the changes in each pathway. Further studies are required to examine the effects of estrogen signaling upon microglial functionality in the healthy brain of both males and females as well as after a TBI.

In conclusion, this study demonstrated microglia undergo temporal changes in phagocytic as well as pro- and anti-inflammatory

proteins following a diffuse TBI. How these temporal changes in the microglia proteome affect recovery post-TBI remains unknown. Therefore, additional studies are required to determine whether microglial proteomic changes correlate with neuropathological and functional outcomes and if effective therapies can be designed to target microglial pathways. Despite the changes in microglial proteins across time post-injury being similar between biological sexes, we reported an increase in pro-inflammatory and phagocytic proteins in naïve and injured males compared with females. Furthermore, naïve and injured males exhibited a greater amount of microglial metabolic signaling proteins which may have implications for endocrine functions that are known to be disrupted after TBI. Lastly, biological sex differences in microglial functionality, regardless of TBI, may impact the effectiveness of treatment strategies targeting the microglial response post-injury.

AUTHOR CONTRIBUTIONS

Dr. Jenna M. Ziebell and Professor Anna E. King conceived the research idea. Dr. Jenna M. Ziebell performed all of the fluid percussion injuries for this work. Yasmine V. Doust collected the tissue, conducted the FACS and immunohistochemistry experiments and prepared the samples for mass spectrometry. Olivia G. Holloway assisted with animal work and FACS experiments. Richard Wilson performed mass spectrometry experiments and wrote the methods for these experiments. Aidan Bindoff conducted the statistical analysis and wrote the methods for this analysis. Yasmine V. Doust wrote an initial draft of the manuscript and formulated the figures and table with input and feedback from all authors. All authors edited and revised the manuscript for final publication. All authors contributed to the article and approved the submitted version.

ACKNOWLEDGMENTS

The authors would like to thank Dr. Terry L. Pinfold and Dr. William R. Bennett for their technical assistance and Dr. Dino Premilovac for his assistance with data interpretation. Research reported in this manuscript was funded by the J.O. and J.R. Wicking Trust. Prof. Anna E. King is supported by an NHMRC boosting dementia research leadership fellowship (APP1136913). Table of contents figure was created with BioRender.com. Open access publishing facilitated by University of Tasmania, as part of the Wiley - University of Tasmania agreement via the Council of Australian University Librarians.

DATA AVAILABILITY STATEMENT

Data sharing is not applicable to this article as no new data were created or analyzed in this study.

ORCID

Jenna M. Ziebell  <https://orcid.org/0000-0003-2497-4347>

REFERENCES

- Abu Hamdeh, S., Shevchenko, G., Mi, J., Musunuri, S., Bergquist, J., & Marklund, N. (2018). Proteomic differences between focal and diffuse traumatic brain injury in human brain tissue. *Scientific Reports*, 8(1), 6807. <https://doi.org/10.1038/s41598-018-25060-0>

- Bachiller, S., Jiménez-Ferrer, I., Paulus, A., Yang, Y., Swanberg, M., Deierborg, T., & Boza-Serrano, A. (2018). Microglia in neurological diseases: A road map to brain-disease dependent-inflammatory response. *Frontiers in Cellular Neuroscience*, 12, 488. <https://doi.org/10.3389/fncel.2018.00488>
- Barud, W., Palusinski, R., Beltowski, J., Wojcicka, G., Myslinski, W., Grzybowski, A., Makaruk, B., Mieczkowska, J., & Mosiewicz, J. (2010). Relation between markers of inflammation and estradiol in older men. *Medical Science Monitor*, 16, Cr593-7.
- Bates, D., Mächler, M., Bolker, B., & Walker, S. (2015). Fitting linear mixed-effects models using lme4. *Journal of Statistical Software*, 67(1), 1-48.
- Bobjer, J., Katrinaki, M., Tsatsanis, C., Lundberg Giwerzman, Y., & Giwerzman, A. (2013). Negative association between testosterone concentration and inflammatory markers in young men: a nested cross-sectional study. *PLoS One*, 8, e61466.
- Bohdanowicz, M., & Fairn, G. D. (2011). Rapamycin-based inducible translocation systems for studying phagocytosis. *Methods in Molecular Biology*, 748, 183-193. https://doi.org/10.1007/978-1-61779-139-0_13
- Boone, D. R., Weisz, H. A., Willey, H. E., Torres, K. E. O., Falduto, M. T., Sinha, M., Spratt, H., Bolding, I. J., Johnson, K. M., Parsley, M. A., DeWitt, D. S., Prough, D. S., & Hellmich, H. L. (2019). Traumatic brain injury induces long-lasting changes in immune and regenerative signaling. *PLoS One*, 14(4), e0214741. <https://doi.org/10.1371/journal.pone.0214741>
- Brabazon, F., Bermudez, S., Shaughnessy, M., Khayrullina, G., & Byrnes, K. R. (2018). The effects of insulin on the inflammatory activity of BV2 microglia. *PLoS One*, 13(8), e0201878. <https://doi.org/10.1371/journal.pone.0201878>
- Bromberg, C. E., Condon, A. M., Ridgway, S. W., Krishna, G., Garcia-Filion, P. C., Adelson, P. D., Rowe, R. K., & Thomas, T. C. (2020). Sex-dependent pathology in the HPA Axis at a sub-acute period after experimental traumatic brain injury. *Frontiers in Neurology*, 11, 946. <https://doi.org/10.3389/fneur.2020.00946>
- Cao, T., Thomas, T. C., Ziebell, J. M., Pauly, J. R., & Lifshitz, J. (2012). Morphological and genetic activation of microglia after diffuse traumatic brain injury in the rat. *Neuroscience*, 225, 65-75. <https://doi.org/10.1016/j.neuroscience.2012.08.058>
- Carroll, E. L., Outtrim, J. G., Forsyth, F., Manktelow, A. E., Hutchinson, P. J. A., Tenovuo, O., Posti, J. P., Wilson, L., Sahakian, B. J., Menon, D. K., & Newcombe, V. F. J. (2020). Mild traumatic brain injury recovery: A growth curve modelling analysis over 2 years. *Journal of Neurology*, 267(11), 3223-3234. <https://doi.org/10.1007/s00415-020-09979-x>
- Carroll, L. J., Cassidy, J. D., Peloso, P. M., Borg, J., von Holst, H., Holm, L., Paniak, C., Pépin, M., & WHO Collaborating Centre Task Force on Mild Traumatic Brain Injury. (2004). Prognosis for mild traumatic brain injury: Results of the WHO collaborating Centre task force on mild traumatic brain injury. *Journal of Rehabilitation Medicine*, 36(43 Suppl), 84-105. <https://doi.org/10.1080/16501960410023859>
- Chaban, V., Clarke, G. J. B., Skandsen, T., Islam, R., Einarsen, C. E., Vik, A., Damås, J. K., Mollnes, T. E., Håberg, A. K., & Pischke, S. E. (2020). Systemic inflammation persists the first year after mild traumatic brain injury: Results from the prospective Trondheim mild traumatic brain injury study. *Journal of Neurotrauma*, 37(19), 2120-2130. <https://doi.org/10.1089/neu.2019.6963>
- D'Andrea, I., Béchade, C., & Maroteaux, L. (2020). Chapter 34 - serotonin and 5-HT2B receptors in microglia control of behavior. In C. P. Müller & K. A. Cunningham (Eds.), *Handbook of behavioral neuroscience* (Vol. 31, pp. 589-599). Elsevier.
- de Freitas Cardoso, M. G., Faleiro, R. M., de Paula, J. J., Kummer, A., Caramelli, P., Teixeira, A. L., de Souza, L. C., & Miranda, A. S. (2019). Cognitive impairment following acute mild traumatic brain injury. *Frontiers in Neurology*, 10, 198. <https://doi.org/10.3389/fneur.2019.00198>
- de la Fuente, A. G., Queiroz, R. M. L., Ghosh, T., McMurran, C. E., Cubillos, J. F., Bergles, D. E., Fitzgerald, D. C., Jones, C. A., Lilley, K. S., Glover, C. P., & Franklin, R. J. M. (2020). Changes in the oligodendrocyte progenitor cell proteome with ageing. *Molecular & Cellular Proteomics*, 19(8), 1281-1302. <https://doi.org/10.1074/mcp.RA120.002102>
- Dhandapani, S., Manju, D., Sharma, B., & Mahapatra, A. (2012). Prognostic significance of age in traumatic brain injury. *Journal of Neurosciences in Rural Practices*, 3(2), 131-135. <https://doi.org/10.4103/0976-3147.98208>
- Doran, S. J., Ritzel, R. M., Glaser, E. P., Henry, R. J., Faden, A. I., & Loane, D. J. (2019). Sex differences in acute Neuroinflammation after experimental traumatic brain injury are mediated by infiltrating myeloid cells. *Journal of Neurotrauma*, 36(7), 1040-1053. <https://doi.org/10.1089/neu.2018.6019>
- Doust, Y. V., Rowe, R. K., Adelson, P. D., Lifshitz, J., & Ziebell, J. M. (2021). Age-at-injury determines the extent of long-term neuropathology and microgliosis after a diffuse brain injury in male rats. *Frontiers in Neurology*, 12(1568). <https://doi.org/10.3389/fneur.2021.722526>
- Fenn, A. M., Gensel, J. C., Huang, Y., Popovich, P. G., Lifshitz, J., & Godbout, J. P. (2014). Immune activation promotes depression 1 month after diffuse brain injury: A role for primed microglia. *Biological Psychiatry*, 76(7), 575-584. <https://doi.org/10.1016/j.biopsych.2013.10.014>
- Galea, O. A., Cottrell, M. A., Treleaven, J. M., & O'Leary, S. P. (2018). Sensorimotor and physiological indicators of impairment in mild traumatic brain injury: A meta-analysis. *Neurorehabilitation and Neural Repair*, 32(2), 115-128. <https://doi.org/10.1177/1545968318760728>
- Gao, Z., Zhu, Q., Zhang, Y., Zhao, Y., Cai, L., Shields, C. B., & Cai, J. (2013). Reciprocal modulation between microglia and astrocyte in reactive gliosis following the CNS injury. *Molecular Neurobiology*, 48(3), 690-701. <https://doi.org/10.1007/s12035-013-8460-4>
- Gehrmann, J., Matsumoto, Y., & Kreutzberg, G. W. (1995). Microglia: Intrinsic immune effector cell of the brain. *Brain Research. Brain Research Reviews*, 20(3), 269-287. [https://doi.org/10.1016/0165-0173\(94\)00015-h](https://doi.org/10.1016/0165-0173(94)00015-h)
- Gentleman, S. M., Leclercq, P. D., Moyes, L., Graham, D. I., Smith, C., Griffin, W. S., & Nicoll, J. A. (2004). Long-term intracerebral inflammatory response after traumatic brain injury. *Forensic Science International*, 146(2-3), 97-104. <https://doi.org/10.1016/j.forsciint.2004.06.027>
- Geric, I., Schoors, S., Claes, C., Gressens, P., Verderio, C., Verfaillie, C. M., van Veldhoven, P. P., Carmeliet, P., & Baes, M. (2019). Metabolic reprogramming during microglia activation. *Immunometabolism*, 1(1), e190002. <https://doi.org/10.20900/immunometab20190002>
- Green, T. R. F., Murphy, S. M., Ortiz, J. B., & Rowe, R. K. (2021). Age-At-injury influences the glial response to traumatic brain injury in the cortex of male juvenile rats. *Frontiers in Neurology*, 12, 804139. <https://doi.org/10.3389/fneur.2021.804139>
- Guneykaya, D., Ivanov, A., Hernandez, D. P., Haage, V., Wojtas, B., Meyer, N., Maricos, M., Jordan, P., Buonfiglioli, A., Gielniewski, B., Ochocka, N., Cömert, C., Friedrich, C., Artiles, L. S., Kaminska, B., Mertins, P., Beule, D., Kettenmann, H., & Wolf, S. A. (2018). Transcriptional and translational differences of microglia from male and female brains. *Cell Reports*, 24(10), 2773-2783. <https://doi.org/10.1016/j.celrep.2018.08.001>
- Gupte, R., Brooks, W., Vukas, R., Pierce, J., & Harris, J. (2019). Sex differences in traumatic brain injury: What we know and what we should know. *Journal of Neurotrauma*, 36(22), 3063-3091. <https://doi.org/10.1089/neu.2018.6171>
- Haas, C. B., de Carvalho, A. K., Muller, A. P., Eggen, B. J. L., & Portela, L. V. (2020). Insulin activates microglia and increases COX-2/IL-1 β expression in young but not in aged hippocampus. *Brain Research*, 1741, 146884. <https://doi.org/10.1016/j.brainres.2020.146884>
- Hanscom, M., Loane, D. J., Aubretch, T., Leser, J., Molesworth, K., Hedgekar, N., Ritzel, R. M., Abulwerdi, G., Shea-Donohue, T., & Faden, A. I. (2021). Acute colitis during chronic experimental traumatic brain injury in mice induces dysautonomia and persistent extraintestinal, systemic, and CNS inflammation with exacerbated neurological



- deficits. *Journal of Neuroinflammation*, 18(1), 24. <https://doi.org/10.1186/s12974-020-02067-x>
- Haure-Mirande, J.-V., Wang, M., Audrain, M., Fanutza, T., Kim, S. H., Heja, S., Readhead, B., Dudley, J. T., Blitzer, R. D., Schadt, E. E., Zhang, B., Gandy, S., & Ehrlich, M. E. (2019). Integrative approach to sporadic Alzheimer's disease: Deficiency of TYROBP in cerebral A β amyloidosis mouse normalizes clinical phenotype and complement subnetwork molecular pathology without reducing A β burden. *Molecular Psychiatry*, 24(3), 431–446. <https://doi.org/10.1038/s41380-018-0255-6>
- Herzog, C., Pons Garcia, L., Keatinge, M., Greenald, D., Moritz, C., Peri, F., & Herrgen, L. (2019). Rapid clearance of cellular debris by microglia limits secondary neuronal cell death after brain injury in vivo. *Development*, 146(9). <https://doi.org/10.1242/dev.174698>
- Holland, R., McIntosh, A. L., Finucane, O. M., Mela, V., Rubio-Araiz, A., Timmons, G., McCarthy, S. A., Gun'ko, Y. K., & Lynch, M. A. (2018). Inflammatory microglia are glycolytic and iron retentive and typify the microglia in APP/PS1 mice. *Brain, Behavior, and Immunity*, 68, 183–196. <https://doi.org/10.1016/j.bbi.2017.10.017>
- Honig, M. G., del Mar, N. A., Henderson, D. L., O'Neal, D., Doty, J. B., Cox, R., Li, C., Perry, A. M., Moore, B. M., & Reiner, A. (2021). Raloxifene modulates microglia and rescues visual deficits and pathology after impact traumatic brain injury. *Frontiers in Neuroscience*, 15. <https://doi.org/10.3389/fnins.2021.701317>
- Hughes, C. S., Moggridge, S., Müller, T., Sorensen, P. H., Morin, G. B., & Krijgsvelde, J. (2019). Single-pot, solid-phase-enhanced sample preparation for proteomics experiments. *Nature Protocols*, 14(1), 68–85. <https://doi.org/10.1038/s41596-018-0082-x>
- Hughes, P. M., Botham, M. S., Frentzel, S., Mir, A., & Perry, V. H. (2002). Expression of fractalkine (CX3CL1) and its receptor, CX3CR1, during acute and chronic inflammation in the rodent CNS. *Glia*, 37(4), 314–327.
- Izzy, S., Liu, Q., Fang, Z., Lule, S., Wu, L., Chung, J. Y., Sarro-Schwartz, A., Brown-Whalen, A., Perner, C., Hickman, S. E., Kaplan, D. L., Patsopoulos, N. A., el Khoury, J., & Whalen, M. J. (2019). Time-dependent changes in microglia transcriptional networks following traumatic brain injury. *Frontiers in Cellular Neuroscience*, 13(307). <https://doi.org/10.3389/fncel.2019.00307>
- Jassam, Y. N., Izzy, S., Whalen, M., McGavern, D. B., & El Khoury, J. (2017). Neuroimmunology of traumatic brain injury: Time for a paradigm shift. *Neuron*, 95(6), 1246–1265. <https://doi.org/10.1016/j.neuron.2017.07.010>
- Johnson, V. E., Stewart, J. E., Begbie, F. D., Trojanowski, J. Q., Smith, D. H., & Stewart, W. (2013). Inflammation and white matter degeneration persist for years after a single traumatic brain injury. *Brain*, 136(Pt 1), 28–42. <https://doi.org/10.1093/brain/aws322>
- Jung, S., Aliberti, J., Graemmel, P., Sunshine, M. J., Kreutzberg, G. W., Sher, A., & Littman, D. R. (2000). Analysis of fractalkine receptor CX(3)CR1 function by targeted deletion and green fluorescent protein reporter gene insertion. *Molecular and Cellular Biology*, 20(11), 4106–4114. <https://doi.org/10.1128/mcb.20.11.4106-4114.2000>
- Kelley, B. J., Lifshitz, J., & Povlishock, J. T. (2007). Neuroinflammatory responses after experimental diffuse traumatic brain injury. *Journal of Neuropathology and Experimental Neurology*, 66(11), 989–1001. <https://doi.org/10.1097/NEN.0b013e3181588245>
- Kofler, J., & Wiley, C. A. (2011). Microglia: Key innate immune cells of the brain. *Toxicologic Pathology*, 39(1), 103–114. <https://doi.org/10.1177/0192623310387619>
- Konopka, T. (2020). UMAP: Uniform manifold approximation and projection. R package version 0.2.7.0. <https://CRAN.R-project.org/package=umap>
- Koussounadis, A., Langdon, S. P., Um, I. H., Harrison, D. J., & Smith, V. A. (2015). Relationship between differentially expressed mRNA and mRNA-protein correlations in a xenograft model system. *Scientific Reports*, 5(1), 10775. <https://doi.org/10.1038/srep10775>
- Kövesdi, E., Szabó-Meleg, E., & Abrahám, I. M. (2020). The role of estradiol in traumatic brain injury: Mechanism and treatment potential. *International Journal of Molecular Sciences*, 22(1), 11. <https://doi.org/10.3390/ijms22010011>
- Krabbe, G., Matyash, V., Pannasch, U., Mamer, L., Boddeke, H. W., & Kettenmann, H. (2012). Activation of serotonin receptors promotes microglial injury-induced motility but attenuates phagocytic activity. *Brain, Behavior, and Immunity*, 26(3), 419–428. <https://doi.org/10.1016/j.bbi.2011.12.002>
- Kumar, A., Alvarez-Croda, D. M., Stoica, B. A., Faden, A. I., & Loane, D. J. (2016). Microglial/macrophage polarization dynamics following traumatic brain injury. *Journal of Neurotrauma*, 33(19), 1732–1750. <https://doi.org/10.1089/neu.2015.4268>
- Kwok, F. Y., Lee, T. M., Leung, C. H., & Poon, W. S. (2008). Changes of cognitive functioning following mild traumatic brain injury over a 3-month period. *Brain Injury*, 22(10), 740–751. <https://doi.org/10.1080/02699050802336989>
- Lafrenaye, A. D., Todani, M., Walker, S. A., & Povlishock, J. T. (2015). Microglia processes associate with diffusely injured axons following mild traumatic brain injury in the micro pig. *Journal of Neuroinflammation*, 12, 186. <https://doi.org/10.1186/s12974-015-0405-6>
- Laskowski, R. A., Creed, J. A., & Raghupathi, R. (2015). Pathophysiology of mild TBI: Implications for altered signaling pathways. In F. H. Kobeissy (Ed.), *Brain Neurotrauma: Molecular, neuropsychological, and rehabilitation aspects*. CRC Press/Taylor & Francis.
- Lauro, C., & Limatola, C. (2020). Metabolic reprogramming of microglia in the regulation of the innate inflammatory response. *Frontiers in Immunology*, 11(493). <https://doi.org/10.3389/fimmu.2020.00493>
- Lenth, R., Buurkner, P., Herve, M., Love, J., Riebel, H., & Singmann, H. (2021). Emmeans: Estimated marginal means, aka least-squares means. R Package Version, 1(5), 5 <https://cran.r-project.org/web/packages/emmeans/index.html>
- Lenz, K. M., Nugent, B. M., Haliyur, R., & McCarthy, M. M. (2013). Microglia are essential to masculinization of brain and behavior. *Journal of Neuroscience*, 33, 2761–2772.
- Li, M., & Sirko, S. (2018). Traumatic brain injury: At the crossroads of neuropathology and common metabolic Endocrinopathies. *Journal of Clinical Medicine*, 7(3). <https://doi.org/10.3390/jcm7030059>
- Li, Q., & Barres, B. A. (2018). Microglia and macrophages in brain homeostasis and disease. *Nature Reviews. Immunology*, 18(4), 225–242. <https://doi.org/10.1038/nri.2017.125>
- Lifshitz, J., & Lisembee, A. M. (2012). Neurodegeneration in the somatosensory cortex after experimental diffuse brain injury. *Brain Structure & Function*, 217(1), 49–61. <https://doi.org/10.1007/s00429-011-0323-z>
- Lifshitz, J., Rowe, R. K., Griffiths, D. R., Evilsizor, M. N., Thomas, T. C., Adelson, P. D., & McIntosh, T. K. (2016). Clinical relevance of midline fluid percussion brain injury: Acute deficits, chronic morbidities and the utility of biomarkers. *Brain Injury*, 30(11), 1293–1301. <https://doi.org/10.1080/02699052.2016.1193628>
- Liu, C., Dai, S. K., Shi, R. X., He, X. C., Wang, Y. Y., He, B. D., Sun, X. W., du, H. Z., Liu, C. M., & Teng, Z. Q. (2021). Transcriptional profiling of microglia in the injured brain reveals distinct molecular features underlying neurodegeneration. *Glia*, 69(5), 1292–1306. <https://doi.org/10.1002/glia.23966>
- Loane, D. J., Kumar, A., Stoica, B. A., Cabatbat, R., & Faden, A. I. (2014). Progressive neurodegeneration after experimental brain trauma: Association with chronic microglial activation. *Journal of Neuropathology and Experimental Neurology*, 73(1), 14–29. <https://doi.org/10.1097/nen.0000000000000021>
- Losoi, H., Silverberg, N. D., Wäljas, M., Turunen, S., Rosti-Otajarvi, E., Helminen, M., Luoto, T. M., Julkunen, J., Öhman, J., & Iverson, G. L. (2016). Recovery from mild traumatic brain injury in previously healthy adults. *Journal of Neurotrauma*, 33(8), 766–776. <https://doi.org/10.1089/neu.2015.4070>

- Luo, W., Yang, Z., Zhang, W., Zhou, D., Guo, X., Wang, S., He, F., & Wang, Y. (2021). Quantitative proteomics reveals the dynamic pathophysiology across different stages in a rat model of severe traumatic brain injury. *Frontiers in Molecular Neuroscience*, 14, 785938. <https://doi.org/10.3389/fnmol.2021.785938>
- Lushchak, V. I., Duzsenko, M., Gospodaryov, D. V., & Garaschuk, O. (2021). Oxidative stress and energy metabolism in the brain: Midlife as a turning point. *Antioxidants*, 10(11). <https://doi.org/10.3390/antiox10111715>
- Madathil, S. K., Wilfred, B. S., Urankar, S. E., Yang, W., Leung, L. Y., Gilsdorf, J. S., & Shear, D. A. (2018). Early microglial activation following closed-head concussive injury is dominated by pro-inflammatory M-1 type. *Frontiers in Neurology*, 9(964). <https://doi.org/10.3389/fneur.2018.00964>
- Maggio, M., Ceda, G. P., Lauretani, F., Bandinelli, S., Metter, E. J., Artoni, A., Gatti, E., Ruggiero, C., Guralnik, J. M., Valenti, G., Ling, S. M., Basaria, S., & Ferrucci, L. (2009). Estradiol and inflammatory markers in older men. *Journal of Clinical Endocrinology & Metabolism*, 94, 518–522.
- Mao, Y., & Finnemann, S. C. (2015). Regulation of phagocytosis by rho GTPases. *Small GTPases*, 6(2), 89–99. <https://doi.org/10.4161/21541248.2014.989785>
- Martin, N. A., Hyrlov, K. H., Elkjaer, M. L., Thygesen, E. K., Włodarczyk, A., Elbaek, K. J., Abo, C., Okarmus, J., Benedikz, E., Reynolds, R., Hegedus, Z., Stensballe, A., Svenningsen, Å. F., Owens, T., & Illes, Z. (2020). Absence of miRNA-146a differentially alters microglia function and proteome. *Frontiers in Immunology*, 11, 1110. <https://doi.org/10.3389/fimmu.2020.01110>
- Matejuk, A., & Ransohoff, R. M. (2020). Crosstalk between astrocytes and microglia: An overview. *Frontiers in Immunology*, 11, 1416. <https://doi.org/10.3389/fimmu.2020.01416>
- McCulloch, C. E., & Neuhaus, J. M. (2014). *Generalized linear mixed models*. Statistics Reference Online. <https://doi.org/10.1002/9781118445112.stat07540>
- McInnes, L., Healy, J., & Melville, J. (2018). UMAP: Uniform manifold approximation and projection for dimension reduction. *arXiv preprint*, arXiv:1802.03426.
- Mikolić, A., van Klaveren, D., Groeniger, J. O., Wieggers, E. J. A., Lingsma, H. F., Zeldovich, M., von Steinbüchel, N., Maas, A. I. R., Roeters van Lennep, J., Polinder, S., & CENTER-TBI Participants and Investigators. (2021). Differences between men and women in treatment and outcome after traumatic brain injury. *Journal of Neurotrauma*, 38(2), 235–251. <https://doi.org/10.1089/neu.2020.7228>
- Moon, J.-S., Nakahira, K., Chung, K.-P., DeNicola, G. M., Koo, M. J., Pabón, M. A., Rooney, K. T., Yoon, J. H., Ryter, S. W., Stout-Delgado, H., & Choi, A. M. K. (2016). NOX4-dependent fatty acid oxidation promotes NLRP3 inflammasome activation in macrophages. *Nature Medicine*, 22(9), 1002–1012. <https://doi.org/10.1038/nm.4153>
- Morganti, J. M., Riparip, L. K., & Rosi, S. (2016). Call off the dog(ma): M1/M2 polarization is concurrent following traumatic brain injury. *PLoS One*, 11(1), e0148001. <https://doi.org/10.1371/journal.pone.0148001>
- Morrison, H., Young, K., Qureshi, M., Rowe, R. K., & Lifshitz, J. (2017). Quantitative microglia analyses reveal diverse morphologic responses in the rat cortex after diffuse brain injury. *Scientific Reports*, 7(1), 13211. <https://doi.org/10.1038/s41598-017-13581-z>
- Mushkudiani, N. A., Engel, D. C., Steyerberg, E. W., Butcher, I., Lu, J., Marmarou, A., Slieker, F., McHugh, G. S., Murray, G. D., & Maas, A. I. R. (2007). Prognostic value of demographic characteristics in traumatic brain injury: Results from the IMPACT study. *Journal of Neurotrauma*, 24(2), 259–269. <https://doi.org/10.1089/neu.2006.0028>
- Nelson, L. D., Temkin, N. R., Dikmen, S., Barber, J., Giacino, J. T., Yuh, E., Levin, H. S., McCrea, M. A., Stein, M. B., Mukherjee, P., Okonkwo, D. O., Robertson, C. S., Diaz-Arrastia, R., Manley, G. T., and the TRACK-TBI Investigators, Adeoye, O., Badjatia, N., Boase, K., Bodien, Y., ... Zafonte, R. (2019). Recovery after mild traumatic brain injury in patients presenting to US level I trauma centers: A transforming research and clinical knowledge in traumatic brain injury (TRACK-TBI) study. *JAMA Neurology*, 76(9), 1049–1059. <https://doi.org/10.1001/jamaneurol.2019.1313>
- Nimmerjahn, A., Kirchhoff, F., & Helmchen, F. (2005). Resting microglial cells are highly dynamic surveillants of brain parenchyma in vivo. *Science*, 308(5726), 1314–1318. <https://doi.org/10.1126/science.1110647>
- Nonaka, M., Taylor, W. W., Bukalo, O., Tucker, L. B., Fu, A. H., Kim, Y., McCabe, J. T., & Holmes, A. (2021). Behavioral and myelin-related abnormalities after blast-induced mild traumatic brain injury in mice. *Journal of Neurotrauma*, 38(11), 1551–1571. <https://doi.org/10.1089/neu.2020.7254>
- Perez-Riverol, Y., Bai, J., Bandla, C., García-Seisdedos, D., Hewapathirana, S., Kamatchinathan, S., Kundu, D. J., Prakash, A., Frericks-Zipper, A., Eisenacher, M., Walzer, M., Wang, S., Buzza, A., & Vizcaíno, J. A. (2022). The PRIDE database resources in 2022: A hub for mass spectrometry-based proteomics evidences. *Nucleic Acids Research*, 50(D1), D543–d552. <https://doi.org/10.1093/nar/gkab1038>
- Prins, M., Greco, T., Alexander, D., & Giza, C. C. (2013). The pathophysiology of traumatic brain injury at a glance. *Disease Models & Mechanisms*, 6(6), 1307–1315. <https://doi.org/10.1242/dmm.011585>
- R Core Team. (2021). *R: A language and environment for statistical computing*. R Foundation for Statistical Computing <https://www.R-project.org/>
- Ramlackhansingh, A. F., Brooks, D. J., Greenwood, R. J., Bose, S. K., Turkheimer, F. E., Kinnunen, K. M., Gentleman, S., Heckemann, R. A., Gunanayagam, K., Gelosa, G., & Sharp, D. J. (2011). Inflammation after trauma: Microglial activation and traumatic brain injury. *Annals of Neurology*, 70(3), 374–383. <https://doi.org/10.1002/ana.22455>
- Rangaraju, S., Dammer, E. B., Raza, S. A., Gao, T., Xiao, H., Betarbet, R., Duong, D. M., Webster, J. A., Hales, C. M., Lah, J. J., Levey, A. I., & Seyfried, N. T. (2018). Quantitative proteomics of acutely-isolated mouse microglia identifies novel immune Alzheimer's disease-related proteins. *Molecular Neurodegeneration*, 13(1), 34. <https://doi.org/10.1186/s13024-018-0266-4>
- Ritzel, R. M., Li, Y., He, J., Khan, N., Doran, S. J., Faden, A. I., & Wu, J. (2020). Sustained neuronal and microglial alterations are associated with diverse neurobehavioral dysfunction long after experimental brain injury. *Neurobiology of Disease*, 136, 104713. <https://doi.org/10.1016/j.nbd.2019.104713>
- Rowe, R. K., Griffiths, D. R., & Lifshitz, J. (2016). Midline (central) fluid percussion model of traumatic brain injury. *Methods in Molecular Biology*, 1462, 211–230. https://doi.org/10.1007/978-1-4939-3816-2_13
- Rowe, R. K., Harrison, J. L., Ellis, T. W., Adelson, P. D., & Lifshitz, J. (2018). Midline (central) fluid percussion model of traumatic brain injury in pediatric and adolescent rats. *Journal of Neurosurgery. Pediatrics*, 22(1), 22–30. <https://doi.org/10.3171/2018.1.Peds17449>
- Rowe, R. K., Harrison, J. L., Morrison, H. W., Subbian, V., Murphy, S. M., & Lifshitz, J. (2019). Acute post-traumatic sleep May define vulnerability to a second traumatic brain injury in mice. *Journal of Neurotrauma*, 36(8), 1318–1334. <https://doi.org/10.1089/neu.2018.5980>
- Rowe, R. K., Rumney, B. M., May, H. G., Permana, P., Adelson, P. D., Harman, S. M., Lifshitz, J., & Thomas, T. C. (2016). Diffuse traumatic brain injury affects chronic corticosterone function in the rat. *Endocrine Connections*, 5(4), 152–166. <https://doi.org/10.1530/ec-16-0031>
- Rowe, R. K., Ziebell, J. M., Harrison, J. L., Law, L. M., Adelson, P. D., & Lifshitz, J. (2016). Aging with traumatic brain injury: Effects of age at injury on behavioral outcome following diffuse brain injury in rats. *Developmental Neuroscience*, 38(3), 195–205. <https://doi.org/10.1159/000446773>
- Rowland, B., Savarraj, J. P. J., Karri, J., Zhang, X., Cardenas, J., Choi, H. A., Holcomb, J. B., & Wade, C. E. (2020). Acute inflammation in traumatic brain injury and Polytrauma patients using network analysis. *Shock*, 53(1), 24–34. <https://doi.org/10.1097/shk.0000000000001349>



- Saba, E. S., Karout, M., Nasrallah, L., Kobeissy, F., Darwish, H., & Khoury, S. J. (2021). Long-term cognitive deficits after traumatic brain injury associated with microglia activation. *Clinical Immunology*, 230, 108815. <https://doi.org/10.1016/j.clim.2021.108815>
- Scott, M. C., Prabhakara, K. S., Walters, A. J., Olson, S. D., & Cox, C. S., Jr. (2022). Determining sex-based differences in inflammatory response in an experimental traumatic brain injury model. *Frontiers in Immunology*, 13, 753570. <https://doi.org/10.3389/fimmu.2022.753570>
- Sharma, R., Zamani, A., Dill, L. K., Sun, M., Chu, E., Robinson, M. J., O'Brien, T. J., Shultz, S. R., & Semple, B. D. (2021). A systemic immune challenge to model hospital-acquired infections independently regulates immune responses after pediatric traumatic brain injury. *Journal of Neuroinflammation*, 18(1), 72. <https://doi.org/10.1186/s12974-021-02114-1>
- Shitaka, Y., Tran, H. T., Bennett, R. E., Sanchez, L., Levy, M. A., Dikranian, K., & Brody, D. L. (2011). Repetitive closed-skull traumatic brain injury in mice causes persistent multifocal axonal injury and microglial reactivity. *Journal of Neuropathology and Experimental Neurology*, 70(7), 551–567. <https://doi.org/10.1097/NEN.0b013e31821f891f>
- Smith, C., Gentleman, S. M., Leclercq, P. D., Murray, L. S., Griffin, W. S., Graham, D. I., & Nicoll, J. A. (2013). The neuroinflammatory response in humans after traumatic brain injury. *Neuropathology and Applied Neurobiology*, 39(6), 654–666. <https://doi.org/10.1111/nan.12008>
- Spielman, L. J., Bahniwal, M., Little, J. P., Walker, D. G., & Klegeris, A. (2015). Insulin modulates in vitro secretion of cytokines and Cytotoxins by human glial cells. *Current Alzheimer Research*, 12(7), 684–693. <https://doi.org/10.2174/1567205012666150710104428>
- Stratoulas, V., Venero, J. L., Tremblay, M., & Joseph, B. (2019). Microglial subtypes: Diversity within the microglial community. *The EMBO Journal*, 38(17), e101997. <https://doi.org/10.15252/embj.2019101997>
- Szklarczyk, D., Gable, A. L., Lyon, D., Junge, A., Wyder, S., Huerta-Cepas, J., Simonovic, M., Doncheva, N. T., Morris, J. H., Bork, P., Jensen, L. J., & Mering, C. v. (2018). STRING v11: Protein–protein association networks with increased coverage, supporting functional discovery in genome-wide experimental datasets. *Nucleic Acids Research*, 47(D1), D607–D613. <https://doi.org/10.1093/nar/gky1131>
- Taib, T., Leconte, C., van Steenwinkel, J., Cho, A. H., Palmier, B., Torsello, E., Lai Kuen, R., Onyeomah, S., Ecomard, K., Benedetto, C., Coqueran, B., Novak, A. C., Deou, E., Plotkine, M., Gressens, P., Marchand-Leroux, C., & Besson, V. C. (2017). Neuroinflammation, myelin and behavior: Temporal patterns following mild traumatic brain injury in mice. *PLoS One*, 12(9), e0184811. <https://doi.org/10.1371/journal.pone.0184811>
- Tremblay, M., Stevens, B., Sierra, A., Wake, H., Bessis, A., & Nimmerjahn, A. (2011). The role of microglia in the healthy brain. *The Journal of Neuroscience*, 31(45), 16064–16069. <https://doi.org/10.1523/jneurosci.4158-11.2011>
- Tyanova, S., Temu, T., Sinitcyn, P., Carlson, A., Hein, M. Y., Geiger, T., Mann, M., & Cox, J. (2016). The Perseus computational platform for comprehensive analysis of (prote)omics data. *Nature Methods*, 13, 731–740.
- van der Naalt, J., van Zomeren, A. H., Sluiter, W. J., & Minderhoud, J. M. (1999). One year outcome in mild to moderate head injury: The predictive value of acute injury characteristics related to complaints and return to work. *Journal of Neurology, Neurosurgery, and Psychiatry*, 66(2), 207–213. <https://doi.org/10.1136/jnnp.66.2.207>
- Villa, A., Gelosa, P., Castiglioni, L., Cimino, M., Rizzi, N., Pepe, G., Lolli, F., Marcello, E., Sironi, L., Vegeto, E., & Maggi, A. (2018). Sex-specific features of microglia from adult mice. *Cell Reports*, 23(12), 3501–3511. <https://doi.org/10.1016/j.celrep.2018.05.048>
- Villapol, S., Loane, D. J., & Burns, M. P. (2017). Sexual dimorphism in the inflammatory response to traumatic brain injury. *Glia*, 65(9), 1423–1438. <https://doi.org/10.1002/glia.23171>
- Wall, E. A., Zavzavadjian, J. R., Chang, M. S., Randhawa, B., Zhu, X., Hsueh, R. C., Liu, J., Driver, A., Bao, X. R., Sternweis, P. C., Simon, M. I., & Fraser, I. D. (2009). Suppression of LPS-induced TNF- α ; production in macrophages by cAMP is mediated by PKA-AKAP95-p105. *Science Signaling*, 2(75), ra28-ra28. <https://doi.org/10.1126/scisignal.2000202>
- Wang, J., Hou, Y., Zhang, L., Liu, M., Zhao, J., Zhang, Z., Ma, Y., & Hou, W. (2021). Estrogen attenuates traumatic brain injury by inhibiting the activation of microglia and astrocyte-mediated Neuroinflammatory responses. *Molecular Neurobiology*, 58(3), 1052–1061. <https://doi.org/10.1007/s12035-020-02171-2>
- Wang, L., Pavlou, S., Du, X., Bhuckory, M., Xu, H., & Chen, M. (2019). Glucose transporter 1 critically controls microglial activation through facilitating glycolysis. *Molecular Neurodegeneration*, 14(1), 2. <https://doi.org/10.1186/s13024-019-0305-9>
- Wickham, H., Navarro, D., & Pedersen, T. L. (2016). *ggplot2: Elegant graphics for data analysis*. Springer-Verlag <https://ggplot2-book.org/>
- Witcher, K. G., Bray, C. E., Chunchai, T., Zhao, F., O'Neil, S. M., Gordillo, A. J., Campbell, W. A., McKim, D. B., Liu, X., Dziabis, J. E., Quan, N., Eiferman, D. S., Fischer, A. J., Kokiko-Cochran, O. N., Askwith, C., & Godbout, J. P. (2021). Traumatic brain injury causes chronic cortical inflammation and neuronal dysfunction mediated by microglia. *The Journal of Neuroscience*, 41(7), 1597–1616. <https://doi.org/10.1523/jneurosci.2469-20.2020>
- Witcher, K. G., Dziabis, J. E., Bray, C. E., Gordillo, A. J., Kumar, J. E., Eiferman, D. S., Godbout, J. P., & Kokiko-Cochran, O. N. (2020). Comparison between midline and lateral fluid percussion injury in mice reveals prolonged but divergent cortical neuroinflammation. *Brain Research*, 1746, 146987. <https://doi.org/10.1016/j.brainres.2020.146987>
- Witcher, K. G., Eiferman, D. S., & Godbout, J. P. (2015). Priming the inflammatory pump of the CNS after traumatic brain injury. *Trends in Neurosciences*, 38(10), 609–620. <https://doi.org/10.1016/j.tins.2015.08.002>
- Witten, D. M., & Tibshirani, R. (2020). PMA: Penalized multivariate analysis. *R Package Version*, 1(2), 1. <https://CRAN.R-project.org/package=PMA>
- Witten, D. M., Tibshirani, R., & Hastie, T. (2009). A penalized matrix decomposition, with applications to sparse principal components and canonical correlation analysis. *Biostatistics*, 10(3), 515–534. <https://doi.org/10.1093/biostatistics/kxp008>
- Wolf, Y., Yona, S., Kim, K. W., & Jung, S. (2013). Microglia, seen from the CX3CR1 angle. *Frontiers in Cellular Neuroscience*, 7, 26. <https://doi.org/10.3389/fncel.2013.00026>
- Xue, J., Zhang, Y., Zhang, J., Zhu, Z., Lv, Q., & Su, J. (2021). Astrocyte-derived CCL7 promotes microglia-mediated inflammation following traumatic brain injury. *International Immunopharmacology*, 99, 107975. <https://doi.org/10.1016/j.intimp.2021.107975>
- Yang, S., Qin, C., Hu, Z.-W., Zhou, L.-Q., Yu, H.-H., Chen, M., Bosco, D. B., Wang, W., Wu, L. J., & Tian, D. S. (2021). Microglia reprogram metabolic profiles for phenotype and function changes in central nervous system. *Neurobiology of Disease*, 152, 105290. <https://doi.org/10.1016/j.nbd.2021.105290>
- Yanguas-Casás, N. (2020). Physiological sex differences in microglia and their relevance in neurological disorders. *Neuroimmunology and Neuroinflammation*, 7, 13–22.
- Yao, H., Coppola, K., Schweig, J. E., Crawford, F., Mullan, M., & Paris, D. (2019). Distinct signaling pathways regulate TREM2 phagocytic and NF κ B antagonistic activities. *Frontiers in Cellular Neuroscience*, 13(457). <https://doi.org/10.3389/fncel.2019.00457>
- Zhang, Z., Yu, J., Wang, P., Lin, L., Liu, R., Zeng, R., Ma, H., & Zhao, Y. (2021). iTRAQ-based proteomic profiling reveals protein alterations after traumatic brain injury and supports thyroxine as a potential treatment. *Molecular Brain*, 14(1), 25. <https://doi.org/10.1186/s13041-021-00739-0>
- Ziebell, J. M., Adelson, P. D., & Lifshitz, J. (2015). Microglia: Dismantling and rebuilding circuits after acute neurological injury. *Metabolic Brain Disease*, 30(2), 393–400. <https://doi.org/10.1007/s11011-014-9539-y>

Ziebell, J. M., Taylor, S. E., Cao, T., Harrison, J. L., & Lifshitz, J. (2012). Rod microglia: Elongation, alignment, and coupling to form trains across the somatosensory cortex after experimental diffuse brain injury. *Journal of Neuroinflammation*, 9, 247. <https://doi.org/10.1186/1742-2094-9-247>

SUPPORTING INFORMATION

Additional supporting information can be found online in the Supporting Information section at the end of this article.

How to cite this article: Doust, Y. V., Bindoff, A., Holloway, O. G., Wilson, R., King, A. E., & Ziebell, J. M. (2023). Temporal changes in the microglial proteome of male and female mice after a diffuse brain injury using label-free quantitative proteomics. *Glia*, 71(4), 880–903. <https://doi.org/10.1002/glia.24313>